Contrasts in chemical composition and oxidative potential in PM10 near flares in oil extraction and refining areas in Ecuador

F. Barraza, G. Uzu, J.-L. Jaffrezo, E. Schreck, H. Budzinski, K. Le Menach, M.-H. Dévier, H. Guyard, A. Calas, M.-I. Perez, et al.

Submitted to Atmospheric Environment

Contrasts in chemical composition and oxidative potential in PM_{10} near flares in oil extraction and refining areas in Ecuador

Barraza, F.[1,§*], Uzu, G.[2,3*], Jaffrezo, J-L.[2], Schreck, E.[1], Budzinski H.[4], Le Menach K.[4], Dévier M-H.[4], Guyard, H.[2], Calas A.[2], Perez, M-I.[5], Villacreces L-A.[5], Maurice, L.[1,6]

[1] Géosciences Environnement Toulouse (GET), Observatoire Midi Pyrénées, Université de Toulouse, CNRS, IRD, 31400 Toulouse, France.
[2] Université Grenoble Alpes, IRD, CNRS, Grenoble INP, IGE, 38058 Grenoble, France.
[3] Universidad Mayor San Andres, Laboratorio de Física de la atmosfera, La Paz, Bolivia.
[4] University of Bordeaux/CNRS, EPOC UMR 5805, LPTC team, 33405 Talence, France.
[5] Empresa Pública de Hidrocarburos del Ecuador EP PETROECUADOR, Área de Gestión Ambiental, P.O Box 17-11-5007/17-11-5008 Quito, Ecuador.
[6] Universidad Andina Simón Bolívar, Área de Salud, P.O. Box 17-12-569, Quito, Ecuador.

***joint corresponding authors:** fiorella.barraza@hotmail.com, gaelle.uzu@ird.fr
[§]Current affiliations: Instituto de Cultivos Tropicales (ICT), Tarapoto, Peru / Department of Renewable Resources, University of Alberta, Edmonton, AB, T6G 2G7, Canada

Abstract

For decades, oil extraction in rural sites in the North Amazon Region (NAR) in Ecuador, have generated mixtures of potentially toxic compounds, such as polycyclic aromatic hydrocarbons (PAHs) and metal(loid)s. The main national refinery and the thermal power plant located in Esmeraldas, on the North Pacific Coast (NPC), are also considered as important sources of air contamination. Particulate matter (PM_{10}) emitted at both sites could induce the formation of reactive oxygen species (ROS) in the lungs upon inhalation and could be associated with respiratory diseases. In this study, PM_{10} mass composition was monitored over a two-year period in both regions: NAR (close to oil platforms and open flares) and NPC (in a public school close to the refinery). PM_{10} composition was assessed in terms of metal(loid)s, organic and elementary carbon (OC, EC), monosaccharides (levoglucosan, mannosan, galactosan), glucose, polyols (sorbitol, mannitol, arabitol), water soluble ions and polycyclic aromatic compounds (PAHs, oxy-PAHs and nitro-PAHs). Additionally, three complementary biochemical and acellular tests were performed to evaluate the oxidative potential (OP).

Results show that the PM_{10} mass and elemental concentrations were higher in NPC than in NAR. Barium and Mo concentrations, commonly used in oil operations, were up to 1000-fold higher than values recorded in other regions of Ecuador. OC/EC ratios and polyols concentrations were higher in NAR than in NPC, indicating a larger biogenic contribution to the PM mass in this region. In NAR, the main sources associated with ROS burden were biogenic emissions and oil production, as indicated by positive correlations between OP, sugars, Ba, some PAHs and oxy-PAHs. On the other hand, in NPC, associations between NH_4^+, Ba, As and Ni imply that oil refining and industrial activities are the main contributors to the OP of PM_{10}.

Keywords: PM_{10}; Ecuador; oil extraction; oil refining; chemical composition; PAHs; Trace metal elements; oxidative potential; air quality.

1. Introduction

Atmospheric pollution has become a growing public health concern and accounts for almost 10% of human mortality worldwide, according to the Environmental Performance Index (EPI, 2016). Indeed, more than 3.5 billion people live in countries with unsafe levels of air pollution (Yang and Wang, 2017). Changes in air quality and climate from local to global scales are influenced by airborne emissions from major urban and industrial areas (Baklanov et al., 2016). Aerosols are composed of particulate matter (PM) and gaseous constituents. Particles are classified according to their aerodynamic diameter as coarse particles (≥ 2.5–10 μm), fine particles (≥ 0.1–2.5 μm) and ultrafine particles or nanoparticles (< 0.1 μm) (Bourdrel et al., 2017). The smaller they are, the deeper they can enter into the respiratory system leading to many health effects, including cancer (Hoek et al., 2013; Raaschou-Nielsen et al., 2013). Depending on the source of emission, PM is composed of many different compounds such as soot, metals and metalloids, salts, PAHs, secondary organic aerosols and even bacterial and fungal products (Santibáñez-Andrade et al., 2017). Agriculture, residential heating and cooking, vehicular traffic, fossil fuel combustion, oil refining, mining, steel industries, marine transport, desert dust and biomass burning are the main anthropogenic sources of outdoor pollution (Gurjar et al., 2016; Hadidi et al., 2016; Liang et al., 2016; Monks et al., 2009).

International air quality standards focus on the quantification of six compounds: ozone, PM, SOx, NOx and Pb. In addition, humans are exposed to other harmful substances such as Cd, As, Ni, Hg, benzo(a)pyrene or benzene (Baldasano et al., 2003; Boyd, 2006; Guerreiro et al., 2014). In front of this major issue, European Union air quality directives are among the most complete and restrictive in the world.

In Latin America, emissions from industrial sectors have experienced rapid growth. However, a lack of air monitoring and/or use of obsolete equipment and questionable methodology, have made the collection of reliable data about air quality difficult (Ossés de Eicker et al., 2010).

Among the well-known sources, crude oil industry generates atmospheric emissions from different sources: gas flaring (Fawole et al., 2016), oil pit evaporation (Avdalović et al., 2016; Kirkhus et al., 2015) and high temperature combustion processes during refining (Yassaa and Cecinato, 2005).

Nowadays, Ecuador is the 5th largest oil producer in South America and the 27th worldwide (Ecuador Oil Production, 2018). Extraction activities have occurred in NAR, while the most important refinery is located in Esmeraldas, along NPC. The Texaco Oil Company operated for 30 years (1960s–1992) in NAR, and technologies used for oil production have generated millions of gallons of untreated toxic waste which were partially released into the environment (Buccina et al., 2013; San Sebastián and Hurtig, 2005). For example, natural gas collected

during oil exploration can be transported and re-used or recycled; however, in developing countries, excess gas is flared or vented *in situ*, being a prominent source of black carbon (BC), the second highest contributor to global warming after CO_2 (Fawole et al., 2016). In the Ecuadorian Amazon, between 1 and 3 million cubic metres of wasted gas was burned daily without temperature or emissions controls (San Sebastián and Hurtig, 2004).

The development of the oil industry, combined with land reform, has significantly contributed to the reduction of tropical forests in Ecuador (Welford and Yarbrough, 2015). For instance, approximately 34% of Amazonian forest has been deforested (Mosandl et al., 2008; Rudel et al., 2002). Even so, the remaining forest acts as an important source of biogenic and anthropogenic aerosol emissions. These sources include high but intermittent biomass burning episodes and a consistent production of primary bioaerosols (i.e., pollen, spores, leaves and soil resuspension) and secondary bioaerosols (low volatile compounds formed in the atmosphere)(Fröhlich-Nowoisky et al., 2016; Martin et al., 2010). In the Amazon, biomass burning includes natural forest fires which are most intense during El Niño events, which are characterised by severe drought and high temperatures (Boy et al., 2008), as well as human-initiated burning for land clearing or land-use change (Artaxo et al., 2013).

Oil production activities, biomass burning and natural biogenic emissions release common contaminants such as PAHs, VOCs, metals and water soluble ions into the atmosphere making source apportionment difficult. However, biomass burning tracers like levoglucosan and its isomers (mannosan and galactosan) are exclusively generated from pyrolysis of cellulose and hemicellulose, the main constituents of plant cell walls (Zhu et al., 2015). The combustion of other materials, such as fossil fuels, does not produce levoglucosan (Cheng et al., 2013). Polyols such as arabitol and mannitol are considered good markers of biogenic emissions and are specifically linked to airborne microorganisms (fungal spores, bacteria) (Fu et al., 2016).

In this context, inhabitants living in regions of the Amazon affected by oil extraction activities or refining may be exposed to a substantial mixture of metal(loid)s and PAHs. However, air quality in Ecuador remains poorly studied (Raysoni et al., 2017) and, to our knowledge, literature about PM_{10} properties and their health impact after inhalation is scarce. In fact, an epidemiological study conducted on a village surrounded by 30 oil wells and 4 powerful gas burners in the Ecuadorian Amazon evidenced that the apparent excess of cancer morbidity and mortality could be linked to the population's exposure to toxic contaminants coming from oil production (San Sebastián et al., 2001). In addition, the origin of the health effects experienced from atmospheric PM is categorised by their ability to induce cellular oxidative stress through generation of ROS in the lung (Idelchik et al., 2017; Secrest et al., 2016). ROS include superoxide radical (O_2•), hydrogen peroxide (H_2O_2), hydroxyl radical (•OH), alkoxyl radical (RO•) and singlet oxygen (O_2) (Hedayat et al., 2015). Quinones and transition metals

have been identified as redox active species able to generate ROS (Charrier and Anastasio, 2012; Crobeddu et al., 2017). This is why the inherent capacity of PM to oxidise a biological media is proposed as a unifying exposure metric to assess health risks from air pollution (Kelly et al., 2012; Sauvain et al., 2013). Several methods coexist for measuring the OP of PM and are based on the depletion of lung anti-oxidants or surrogates when in contact with PM (Borm et al., 2006; Calas et al., 2018, 2017; Huang et al., 2016).

This study, conducted in the centre of oil extraction and refining activities in the Ecuadorian NAR and NPC regions aims to survey the air quality and its evolution over two sampling years. A detailed PM_{10} speciation was achieved and its potential link with oil activities (extraction and refining) was investigated by targeting specific tracers of industrial oil processes. Moreover, we determined the ability of PM to induce ROS formation in the lungs, a key parameter for health impact.

2. Materials and methods

2.1 Description of the study area

Three provinces of Ecuador were selected for this study: Orellana and Sucumbíos located in NAR and Esmeraldas located in NPC, both areas are impacted by oil extraction and oil refining, respectively (Fig. 1). Within each province, one site (house or school) was chosen based on its proximity to oil facilities: Auca Sur (NAR 1: S 0° 42' 16.49'', W 76° 53' 15.96'') and Shuara 9 (NAR 2: N 0° 3' 33.26'', W 76° 33' 37.01''), both 300 m away from gas-burning open flares, and La Florida (NPC: N 0° 55' 54.21'', W 79° 40' 40.91'') 1000 m away from the National Oil Refinery.

Several criteria such as records of oil spills, dumping of formation waters and hotspot maps of air quality were evaluated prior to site selection. This information was collected from the Intelligence Subsystem of Environmental Statistics of Productive Activities in Ecuador (SIESAP, 2015), from surveys conducted in the frame of the MONOIL Research Program "Monitoring of Oil activities in Ecuador: a cross-disciplinary approach between Environment, Health and People" or provided by the National Oil Company (EP PetroEcuador, 2013).

Regarding meteorological conditions, the predominant wind direction was north-northeast and south-southwest in Orellana and Sucumbíos, respectively (INAMHI, 2015). In Esmeraldas, the wind direction was south-southeast and south-southwest, following the Teaone and Esmeraldas rivers towards the Pacific Ocean in the morning; in the afternoon, the wind comes from the ocean and the refinery (EP PetroEcuador, 2013).

The wet season in NPC usually lasts from mid-December until May and the dry season from June until mid-November (GADPE, 2017). In contrast, in the Amazon region, precipitation is continuous throughout the year, but more pronounced between June and September (INAMHI,

2015). Total annual precipitation in both areas can reach more than 3000 mm (between 200 and 500 mm per month). Annual mean temperature is around 25 °C, ranging from 13 up to 38 °C (Pourrut, 1995).

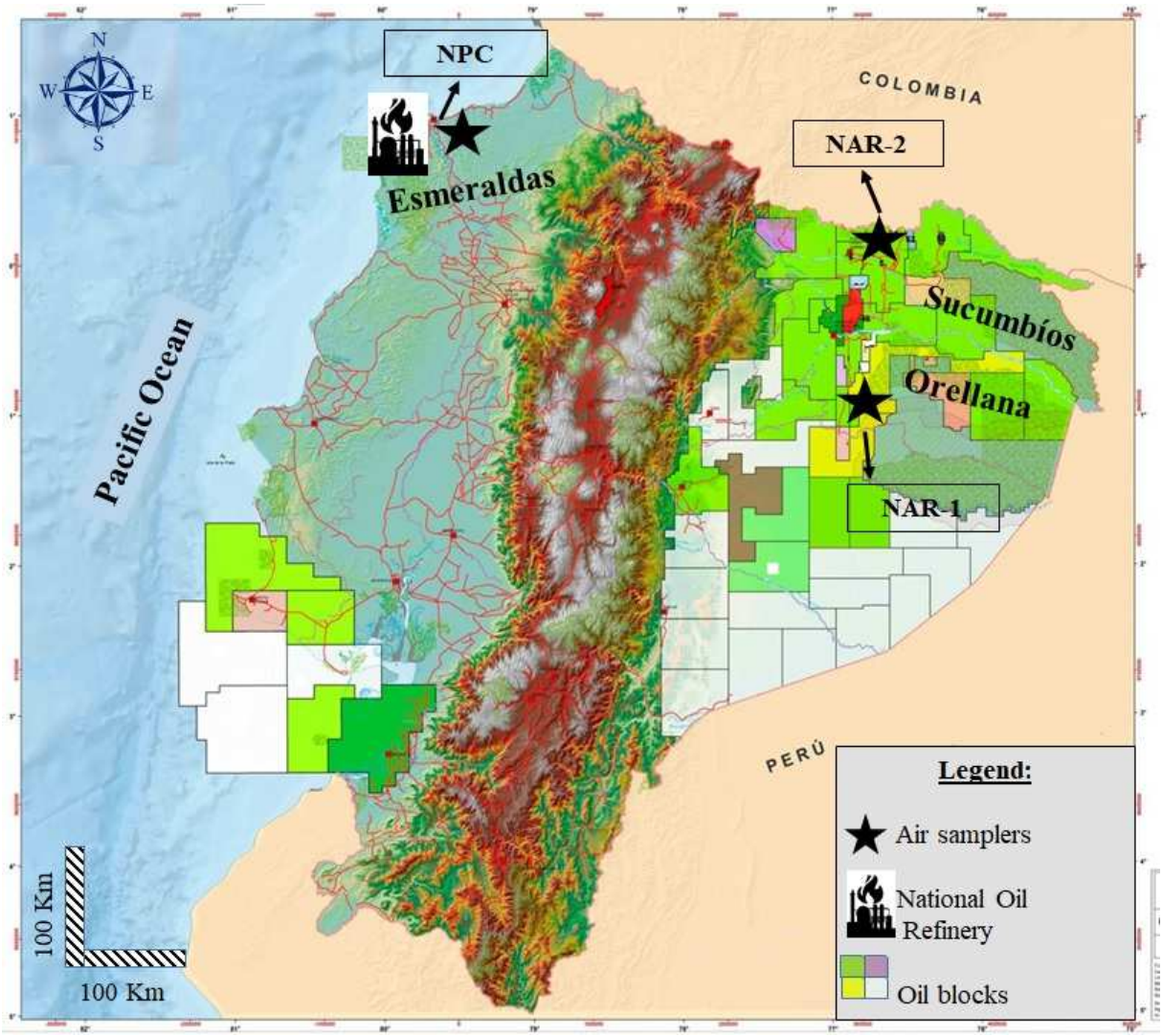

Fig 1. Sampling sites in Orellana (Auca, NAR-1) and Sucumbios (Shuara, NAR-2) provinces in the North Amazon Region and in Esmeraldas (La Florida) on the North Pacific Coast. According to the Ministry of Non-renewable Resources of Ecuador (SHE, 2015), the white blocks have not been assigned to oil exploitation, the others are currently being exploited by different companies (indicated by colors).

2.2 Sampling strategy

PM_{10} and its gas phase (outdoor samples) were collected on quartz fibre filters and polyurethane foams (PUFs; 75 x 25 mm, Tisch Environmental) every two weeks in NPC (12 h per day) and monthly in NAR 1 and 2 (24 h) from January 2015 until December 2016.

Prior to sampling, filters were calcinated at 450 °C for 6h and PUFs were pre-cleaned with dichloromethane by pressurised solvent extraction (ASE; Thermo Scientific Dionex ASE 350) (three extraction cycles, 90 °C, 100 bars, 5 min heat time, 6 min static time and 2 min purge).

Filters and PUFs were wrapped in aluminium foil and, after sampling, they were individually sealed in low-density polyethylene bags.

In total, six one-stage low-volume air samplers (MicroVol-1100) operated at a flow rate of 3 L min^{-1} were settled by pairs on the roof of houses (NAR 1 and 2) or outside an open window grate in a primary school (NPC). Air samplers were powered with solar panels connected to a rechargeable battery pack in NAR 1 and 2 because no electricity was available; and plugged into the electric service in NPC.

During collection and before analysis, PM_{10} samples were protected from the light with aluminum foil, frozen at -5 °C, transported to France in a cooler with dry ice blocks and stored at -20 °C until analysis. Filters were weighed before and after sampling using an electronic microbalance (Mettler Toledo, ±10 µg), previously equilibrated over 24 h in a conditioning chamber until reaching ambient temperature and relative humidity in the clean lab (near 20 °C and not less than 40%, respectively).

2.3 Aerosols chemical composition

2.3.1 Major and trace element concentrations

PM_{10} samples (0–10 µm) impacted on quartz fibre filters (punches of 5 cm^2) were digested on a hot plate using 9 ml of aqua regia, 1 ml of H_2O_2 and 2 ml of HF (trace metal grade analysis, Sigma-Aldrich®). Mineralization solutions were evaporated at 60 °C, the dry residue was then resuspended adding 0.5 ml of HNO_3 and diluted with ultra-pure water before ICP-MS (Agilent 7500 and ICP-MS iCAP Q Thermo Scientific) analyses in order to determine elementary concentrations (adapted from Schreck et al., 2016).

Certified reference material SRM 1648a “Urban Particulate Matter” (from NIST) was used to validate the mineralization method. Recoveries of 80–105% were calculated for all trace metals. Field blank filters and blank acid samples were included on each batch of analyses to eliminate the quartz matrix effect (Table SI-1, Supplementary Information).

2.3.2 Soluble ions

Water soluble cations ammonium (NH_4^+), potassium (K^+), sodium (Na^+), magnesium (Mg^{2+}), calcium (Ca^{2+}) and anions nitrate (NO_3^-), sulfate (SO_4^{2-}), chloride (Cl^-), oxalate $(COO)_2^{2-}$ and methanesulfonate ($MeSO_3^-$) were analyzed by ion chromatography (Dionex ICS-300) on a 4 cm^2 filter punch after extraction in 15 ml of Milli-Q Water. This technique is based on the separation of different ionic species in aqueous solution on an ion exchange resin, using KOH and MSA (methanesulfonic acid) as eluents, followed by the quantification of each one by conductivity detection.

2.3.3 Organic and elementary carbon (OC, EC)

Carbonaceous material was quantified by a thermal-optical analyzer (Sunset Laboratory, EUSAAR2 method®) separating the OC from the EC in the same sample. To separate the two fractions, a punch of 1 cm^2 was heated at different temperature ramps (up to 850 °C) in more or less oxidizing atmospheres. Total carbon (TC) was calculated as the sum of OC and EC.

2.3.4 Organic compounds

Monosaccharide anhydrides (levoglucosan, mannosan, galactosan), polyols (arabitol, mannitol, sorbitol), and sugars (glucose) were analyzed in a 4 cm^2 filter punch, using NaOH as eluent and liquid chromatography-pulsed amperometric detection (LC-PAD, Dionex DX 500®) as described elsewhere (Samaké et al., 2019b, 2019a).

It is important to note that low-volume air samplers (connected to solar panels and batteries) and the one-month sampling protocol must have led to the degradation of the aforementioned compounds towards secondary species and thus, could have led to underestimation.

Quantification limits for each analysis are presented in Table SI-1 (Supplementary Information).

2.3.5 Polycyclic aromatic compounds (PACs)

Parent PAHs, oxygenated-PAHs (oxy-PAHs) and nitrated-PAHs (nitro-PAHs) were determined in both particulate (quartz filters) and gas (PUFs) phases. All monitored PACs and their respective surrogate standards are listed in Table SI-2 (Supplementary Information).

The PAH, oxy-PAH and nitro-PAH analytical procedures were adapted from previous works (Albinet et al., 2006; Perraudin et al., 2005). Briefly, quartz fiber filters and PUFs were spiked with the surrogate standards (9, 7 and 3 perdeuterated congeners of PAHs, nitro-PAHs and oxy-PAHs, respectively) prior to extraction. Two types of quality controls were performed for each series of extraction: a laboratory blank and a control filter/PUF (spiked at low level with analytes and related surrogates) underwent the entire analytical procedure in order to check background contamination and analytical performance (accuracy).

Both filters and PUFs were individually extracted by ASE Thermo Scientific ASE 350, Dionex, France) with dichloromethane (3 extraction cycles, 90 °C, 100 bars, 5 min heat time, 6 min static time and 2 min purge). Extracts were purified through alumina (aluminium oxide 150 basic, 0.063–0.200 mm, Merck) micro-columns with 3 x 5 mL of dichloromethane in order to remove all macromolecules and polar interfering compounds. Extracts were divided into two weighed aliquots: one for the nitro- and oxy-PAHs (aliquot 1) and the other for PAH

determination (aliquot 2), and then reduced to about 500 µL using a RapidVap® vacuum evaporator (Labconco, Kansas City, MO, USA) (50 °C, 900 mbars, 40% speed). Regarding extracts for nitro- and oxy-PAHs (aliquot 1), they were then concentrated to 100 µL dichloromethane under a gentle flow of ultrapure nitrogen (TS2B Toulemonde, Mery-sur-Oise). After the addition of a few µL of isooctane, extracts for PAHs (aliquote 2) in filter samples were evaporated (near to dryness at 45 °C) under a gentle flow of ultrapure nitrogen, and reconstituted in 100 µL isooctane; whereas extracts of PUF samples were further purified on silica micro-columns to separate the alkane fraction from the aromatic one in order to keep a clean GC/MS injection port. Alkanes were desorbed using *n*-pentane, then PAHs were eluted with a 65/35 *n*-pentane/dichloromethane mixture. Finally, the pyrene-d10 and benzo[b]fluoranthene-d12 internal solution was gravimetrically added to all the final extracts for recovery control of surrogate standards.

The 21 parent PAHs were determined by gas chromatography/mass spectrometry using electron ionisation (GC/EI-MS) (7890A GC and 5975C MSD, Agilent Technologies). PAHs were separated at 1.3 mL/min (Helium 6.0, Linde Gas s.a., Bassens, France) on a HP5MS-UI column (30 m x 0.25 mm x 0.25 µm, Agilent Technologies) with the following oven temperature program: 50 °C (2 min) - 10 °C/min - 250 °C (5 min) - 2 °C/min - 280 °C (2 min) - 10 °C/min - 310 °C (3 min). The injection volume was 1 µL (pulsed splitless mode: 25 psi for 1.5 min) and the injector temperature was 280 °C. MS parameters were set as follows: source and quadrupole temperatures: 300 and 180 °C, respectively; electron energy: 70 eV; ions monitored in SIM mode: molecular ions of each native and perdeuterated PACs (dwell time: 30 ms).

The 20 nitro-PAHs and the 10 oxy-PAHs were determined by GC-MS using negative ion chemical ionisation (GC/NICI-MS) (7890A GC and 5975C MSD, Agilent Technologies) with selected ion monitoring (SIM) mode. Nitro- and oxy-PAHs were separated at 1.5 mL/min (helium 6.0, Linde Gas, s.a.) in an OPTIMA-5MS column (30 m x 0.25 mm x 0.25 µm, Macherey-Nagel) with the following oven temperature program: 40 °C (1.6 min) - 45 °C/min - 150 °C (5 min) - 5 °C/min - 300 °C (5 min). Injection was performed with a programmable temperature vaporising (PTV) inlet using the following parameters: temperature from 40 °C (1min) to 280 °C (5 min) at a rate of 10 °C.min^{-1}; purge time: 2 min at 100 mL.min^{-1}. The MS parameters were set as follows: transfer line and source temperatures: 250 and 150 °C, respectively; electron energy: 200 eV; emission current: 150 µA; reagent gas: methane (4.5) at a flow rate of 60%; ions monitored in SIM mode: molecular ions of each native and perdeuterated PACs (dwell time: 100 to 250 ms depending on the compound).

PACs were quantified by their perdeuterated surrogate standards using their molecular ions (SIM mode). Whole-method accuracy was determined on spiked samples (at about 10–20

306 ng/filter or 30–60 ng/PUF) and remained generally between 77–110% for PAHs and 65–135%
307 for nitro-PAHs and oxy-PAHs (except for two of them). Limits of quantification (LOQ) were
308 determined from a 10 signal-to-noise ratio (SNR) observed in low-spiked samples and
309 extrapolated for an air sample volume of 100 m^3 that typically ranged from 0.1 to 10 $pg.m^{-3}$,
310 although higher for a few compounds present in field PUF blanks.
311

312 **2.4 Oxidative potential (OP) of PM_{10}**

313 The OP was assessed through three complementary acellular assays: DTT (dithiothreitol), AA
314 (ascorbic acid) and DCFH (dichlorofluorescin). Extraction of PM from the substrate (filters) for
315 OP assays are usually performed in water, methanol or dichloromethane (Eiguren-Fernandez
316 et al., 2010; Yang et al., 2014). However, to mimic physiological processes when PM enters in
317 contact with lungs, it is suitable to use a medium close to the human respiratory lining fluid—
318 an important interface between inspired air and respiratory tract cells (Schock et al., 2004;
319 Visentin et al., 2016). For this purpose, a Gamble solution supplemented with surfactants such
320 as dipalmitoylphosphatidylcholine (DPPC) was used according to Boisa et al. (2014).
321 Samples (punches of around 0.5 cm^2) were extracted according to Calas et al. (2017) in the
322 Gamble + DPPC solution as described in Section 1 and Table SI-3 (both in Supplementary
323 Information) to reach a constant volume of PM extracted from the solution (25 µg ml^{-1} based
324 on filter surface and PM mass) and vortexed for 75 min at 37 °C. To take into account potential
325 turbidity or intrinsic absorbance of particles, before starting the assay, depletion intrinsic
326 absorbance was determined for every sample (from each well) by spectrophotometry (using
327 TECAN spectrophotometer Infinite® M 200 pro), and then subtracted from measurements.
328 Blank filters were also extracted in the same solution.
329

330 ***2.4.1 Dithiothreitol (DTT) assay* (OP^{DTT})**

331 DTT consumption by formation of DTT-disulfide in the presence of ROS (Yang et al., 2014)
332 was measured in a 96 well CELLSTAR® multiwall plates from Greiner Bio-One®. For each
333 sample, 40 µL of PM extraction (in triplicate) with 205 µL of phosphate buffer (pH=7.4) were
334 incubated at 37 °C in 12.5 nmol of DTT (DTT solution in phosphate buffer). Reaction was
335 stopped at 0, 15 and 30 minutes adding 50 nmol of 5,5'-dithiobis (2-nitrobenzoic acid) (DTNB
336 in phosphate buffer). A solution of 40 µL of 1,4 naphtoquinone (1,4-NQ 24.7 µM) was used a
337 positive control. DTT loss after DTNB titration was read at 412 nm. The OP was obtained from
338 the slope of the linear regression of the consumed DTT (corrected from blank measurements
339 and from intrinsic absorbance of particles) normalized by the PM_{10} air volume (nmol DTT min^{-1} m^{-3}).
340
341

2.4.2 Ascorbic acid (AA) assay (OP^{AA})

Depletion of AA by ROS production when in contact with PM was monitored at 265 nm. Eighty µL of PM extraction and 120 µL of water were injected manually in each well of the Greiner UV-Star® (UV transparent) 96 well plate. Absorbance was read at 265 nm every 4 min for 32 min after injection of 24 nmol of AA (100 µL of AA solution in Milli-Q water). The 1,4 naphtoquinone (NQ) was used as a positive control (Calas et al., 2018)

The AA loss rate (nmol.min^{-1}) was determined from the slope of the linear regression of the calculated nmol of consumed AA *vs* time (corrected for blank and matrix). Units of OP^{AA} were calculated in the same manner as for OP^{DTT}.

2.4.3 Dichlorofluoresceine (DCFH) assay (OP^{DCFH})

The oxidation of DCFH with horseradish peroxidase (HPR) by ROS and the formation of its fluorescent product 2′,7′-dichlorofluorescein (DCF) was measured every minute for 15 min by fluorescence (470 nm excitation/530 nm emission) (Foucaud et al., 2007).

In brief, 40 µL of sample extraction in Gamble + DPPC solution with 220 µL of HRP/DCFH (5 U ml^{-1} and 40 µM respectively, in phosphate buffer) were injected in each well of the ROTH® 96 black multiwall plates. A solution of H_2O_2 at different concentrations (20, 40, 60, 100, 200 and 300 nM), 50 nM of H_2O_2 (used as a positive control) and two blanks of Milli-Q water were included on each batch in order to calibrate the formation rate of superoxide anions, expressed as nmol [H_2O_2] eq. m^{-3}. Detection limits (DL) for each analysis are summarized in Table SI-4 (Supplementary information).

2.5 Mass reconstruction

Reconstructed mass of PM is usually expressed as the sum of its representative chemical components: organic matter (OM), EC, inorganic ions, soil minerals, salts (sea salts near oceans), trace elements and the remaining mass (Chow et al., 2015). General equations used in this study were adapted from methodology developed by Chow et al. (2015), Guinot et al. (2007) and Amato et al. (2016) in agreement with the environmental parameters of the sites:

$$PM_{10}\ \mu g.m^{-3} = OM + EC + (\sum ions) + Soil\ elements + Trace\ metals \quad (1)$$

where:

OM = $\boldsymbol{f}$ x OC, with f = 1.7

OC = organic carbon

∑ions = anions + cations + sea salts (only for NPC)

Soil elements = 1.15 x (3.79 Al + 2.14 Si + 1.67 Ti) + Fe

The conversion factor **(*f*)** to transform OC in OM depends on the production of primary organic aerosol (by combustion sources), the extent of OM oxidation and the formation of secondary organic aerosol (SOA) from anthropogenic or biogenic sources (Chow et al., 2015; Philip et al., 2014). Values for ***f*** can vary from 1.2 in fresh aerosol from urban areas to 2.6 in aged aerosol (Chow et al., 2015; Dai et al., 2018). The ***f*** values (up to 1.6) are commonly applied to oxygenated and/or functionalized organic species that can be expected in emissions from oil activities. Thus, for this study we assumed ***f*** = 1.7.

Because the NPC sampling station was located 5 km from the seashore, sea salts (ss) were also added to Equation 1 (included within "∑ions"), as proposed by Amato et al. (2016):

$$\sum \text{sea salt (ss)} = \text{ssNa} + \text{ssCa} + \text{ssK} + \text{ssMg} + \text{ssSO}_4^{2-} \qquad (2)$$

where:

ssNa = Na - nssNa (=0.348Al); ssCa = 0.038 ssNa; ssK = 0.037 ssNa; ssMg = 0.119 ssNa and ssSO_4^2 = 0.253 ssNa

**nss (non-sea salt).*

2.6 Statistical analyses

The software R® version 3.1.1 was used for all statistical analyses. The non-parametric Spearman correlation (rs) with a level of significance set at 5% (p-value 0.05), based on rank and not dependent on data distribution, was chosen for the regression analyses to measure the strength and relationship between OP and the chemical composition of PM_{10} for each sampling site.

Correlation degree was interpreted as follows:

- Less than 0.40: weak
- 0.41–0.60: moderate
- 0.61–0.79: strong
- 0.79–1: very strong.

3. Results

3.1 PM_{10} mass in oil production and refining areas

PM_{10} contents over two years of sampling in NAR (1 and 2) and in NPC are presented in Table 1 as annual mean concentrations ± standard deviation (SD). In 2015 and 2016, PM_{10} mass concentration in the oil production area was slightly higher in NAR-2 than in NAR-1, reaching values of 27.2 ± 8.3 (2015) and 25.3± 9.6 µg m^{-3}. In NPC (oil refining area), concentrations

were two to four times higher than in NAR, exceeding the European and Ecuadorian legislation limits of 40 and 50 µg m^{-3}, respectively (Table SI-5). In 2015, PM_{10} mean concentration was lower than in 2016 because the refinery was not operating at full capacity.

Regarding monthly and seasonal variations (Fig. SI-1, Supplementary Information), PM_{10} mean concentration in the wet season was 1.6 times lower than in the dry season, but only in NAR-2. In the case of NAR-1, PM_{10} remained similar in both seasons whereas the concentration was slighty higher in NPC in the dry season (Fig. SI-1). However, these apparent seasonality patterns have to be interpreted carefully as there were several samples missing and other technical issues occurred at the three sampling stations (Table 1).

3.2 Elemental and ionic species concentration

Mean concentrations of major elements in NAR (Al, Ca, Fe, Na, Si) ranged between 300 and up to 10 000 ngm^{-3}, two to four times lower than in NPC (Table 1). Trace elements have been classified into four categories according to their concentrations. The first one is represented by Ti and Mo, with annual mean concentrations varying from 36 to 60 and from 56 to 227 ng m^{-3} in NAR and NPC, respectively. Barium, Zn and Cr were part of the second group, with annual mean concentrations ranging from 3 to 33 ng m^{-3} in NAR and from 22 to 95 ng m^{-3} in NPC.

Table 1. Annual chemical composition of PM_{10} in the three sampling sites of Ecuador: NAR-1 (Auca in Orellana) and NAR-2 (Shuara in Sucumbíos), both in NAR and NPC (La Florida in Esmeraldas).

Sampling site	**NAR-1**		**NAR-2**		**NPC**	
N° of Samples*	**N=11**	**N=9**	**N=12**	**N=10**	**N=9**	**N=23**
Year	**2015**	**2016**	**2015**	**2016**	**2015**	**2016[a]**
PM_{10}	23.7±8.6	23.3±8.2	27.2±8.3	25.3±9.6	51.6±23.4	107.2±40.4
Na	7785±1601	1451±3068	10260±1887	247±145	41150±5263	10549±17954
Al	2144±400	1089±686	2525±605	868±567	10347±1139	2620±3231
Ca	3575±664	859±1341	4266±526	219±175	17144±1249	3972±6639
Si	1455±266	1423±266	1816±736	1783±749	8354±2824	8393±2423
Fe	436±133	310±235	472±236	387±247	1308±131	577±174
Ti	41.92±9.25	35.67±24.01	60.91±34.50	46.15±27.85	196.44±194.03	51.83±14.37
Mo	49.00±11.10	38.80±8.21	59.37±8.07	43.13±7.51	226.67±24.79	225.97±60.40
Ba	16.92±3.76	22.09±8.13	14.75±5.37	29.36±6.80	61.04±42.47	94.60±42.05
Zn	14.72±5.58	17.32±7.77	32.53±24.40	24.22±5.65	56.50±39.50	75.95±36.95
Cr	16.91±6.90	4.19±4.48	24.06±2.18	2.48±1.06	61.39±5.73	21.75±20.71
Mn	9.75±2.29	6.09±4.01	9.98±3.24	6.89±3.95	30.25±15.98	11.56±5.45
V	4.13±1.75	5.60±5.37	4.53±1.65	6.75±3.93	22.10±6.87	31.83±10.09
Ni	3.51±1.26	3.76±2.53	4.37±1.29	4.39±2.09	16.59±3.93	19.98±3.84
Sn	3.21±0.71	1.23±1.97	4.49±0.81	0.37±0.18	16.76±2.63	5.97±8.16
Cu	2.19±0.85	1.05±0.72	3.39±2.52	1.41±0.82	10.65±8.89	3.81±1.86
Pb	1.26±0.38	0.52±0.11	2.62±1.86	0.61±0.37	8.11±4.09	2.16±0.82
As	0.60±0.33	0.24±0.17	0.63±0.34	0.37±0.16	2.60±1.41	1.81±1.03
Sb	0.54±0.15	0.29±0.23	0.58±0.14	0.31±0.22	2.76±1.17	1.74±1.12
U	0.45±0.08	0.21±0.18	0.57±0.07	0.14±0.06	2.10±0.24	1.00±0.81
Co	0.26±0.06	0.17±0.11	0.52±0.35	0.18±0.10	0.90±0.25	0.40±0.21
Cd	0.11±0.02	0.09±0.06	0.17±0.09	0.11±0.07	0.44±0.13	0.41±0.26
SO_4^{2-}	1109±524	997±705	731±555	804±557	2556.±737	3119±909.

NO_3^-	72±38	32±31	198±165	24±17	764±570	774±369
$(COO)_2^{2-}$	59±38	35±18	42±25	33±22	201±178	432.±240
Cl^-	13±14	46±68	413±616	15±13	732±473	697±306
$MeSO_3^-$	3±2	4±3	4.±2	4±2	18±14	43±30
Na^+	311.67±102.04	104.00±104.18	685.50±604.47	41.78±43.24	1486.15±1150.06	1158.99±460.05
K^+	224.04±83.76	220.24±185.34	257.56±167.53	191.94±122.52	190.26±70.09	200.68±42.10
NH_4^+	81.41±68.56	167.64±117.76	165.63±150.05	135.15±120.96	231.59±151.86	380.89±181.14
Ca^{2+}	155.52±55.98	60.50±45.14	139.61±173.35	49.19±43.34	472.72±284.36	315.12±138.85
Mg^{2+}	23.48±8.37	23.42±18.88	16.58±8.06	13.17±8.35	76.55±44.23	107.22±36.77
EC	1.07±0.44	1.12±0.89	0.94±0.21	0.74±0.20	0.97±0.32	0.99±0.21
OC	4.58±1.57	5.05±3.67	4.89±1.30	4.44±1.34	3.37±0.72	2.79±0.72
OC/EC	4.56±1.15	4.56±1.58	5.48±1.98	5.99±1.06	3.59±0.49	2.91±0.80
Levoglucosan	4.67±2.25	31.48±10.49	8.35±4.87	56.58±33.80	19.33±12.89	50.83±27.09
Galactosan	<DL	2.55±0.85	0.80±0.53	1.60±0.51	0.59±0.54	1.88±1.16
Mannosan	4.04±2.81	45.66±15.22	0.63±0.38	5.83±3.21	3.81±1.38	5.82±3.47
Glucose	54.86±36.19	54.58±60.71	35.53±32.63	56.79±40.80	33.30±18.84	30.25±20.49
Manitol	151.56±63.47	175.12±144.64	59.20±86.24	134.49±46.30	63.62±31.02	46.77±33.76
Arabitol	50.70±23.43	48.27±44.98	43.40±82.46	34.26±13.59	45.71±24.10	29.93±21.03
Sorbitol	5.46±3.19	2.08±1.48	2.15±1.74	3.63±2.16	6.85±3.80	4.29±2.87
Particulate phase						
∑PAHs-PM[b]	123.1±43.9	316.4±330.1	44.6±35.5	190.6±402.3	790.0±566.5	1192±885.3
∑oxy-PAHs-PM	641±898	333±270	64±87	139±221	1529±1213	844±1045
∑nitro-PAHs-PM	2.4±0.9	2.4 ±1.4	1.4±2.0	0.8±1.1	2.9±0.5	5.3±39
Gas phase						
$\sum PAHs_{-gas}$	2632±1529	--	4215±2056	--	27492±8875	34469±4808
∑oxy-PAHs-gas	551±350	--	1068±388	--	4470±1958	6208±966
∑nitro-PAHs-gas	10±6.4	--	46±48	--	96±54	157±72

Units: mean concentrations of elements and ions (± SD) expressed in ng m^{-3}. PM_{10} mass, EC and OC are expressed in µg m^{-3} and PACs (∑PAHs, ∑oxy-PAHs, and ∑nitro-PAHs) in pg m^{-3}.
*Number of samples was not the same due to several technical issues (e.g., lost samples, broken air samplers)
[a]National Oil refinery operated with only 9 smokestacks in January 2015 and 18 (full capacity) since December 2015.
[b]∑PAHs refers to 15 compounds classified as carcinogenic by the US-EPA (NTP, 2016). Chrysene and triphenylene were included in this sum (see Table SI-2, Supplementary Information). Oxy- and nitro-PAHs are also listed in Table SI-2.
-- No samples collected during this period.
Ambient temperature during sampling ranged between 32 and 38 °C.

The third group, ranging from 1.7 to 29 ng m^{-3}, corresponds to Mn, V, Ni, Sn and Cu. Finally, Pb, As, Sb, U, Co and Cd comprise the fourth group, with concentrations below 3 and 8 ng m^{-3} in NAR and NPC, respectively. For trace elements regulated by Ecuadorian (Cd) and European (As, Cd, Ni and Pb) legislation, concentrations remained below the thresholds (Table SI-5) during the two years of sampling for all sites except for Ni in NPC (25 ngm^{-3} in July 2016). Cation concentrations in NPC are ranked in the following order: $Na^+ > Ca^{2+} > NH_4^+ > K^+ > Mg^{2+}$, whereas in NAR-1 and NAR-2 the order is $K^+ > Na^+ > NH_4^+ > Ca^{2+} > Mg^{2+}$ and $Na^+ > K^+ > NH_4^+ > Ca^{2+} > Mg^{2+}$, respectively.

Among the water soluble anions, SO_4^{2-} and NO_3^- showed the highest mean concentrations in NAR and NPC, ranging from 24 to 3119 ng m^{-3}. Sulfates, Cl^- and $(COO)_2^{2-}$ concentrations in NPC were between 2 and 16 times higher than in the NAR area.

459

460 **3.3 Organic components, sugars and polyols composition of PM_{10}**

461

462 In NAR 1 and 2, OC/EC ratios were similar, ranging from 3 to 10, but higher than those
463 calculated for NPC as can be seen in Fig. SI-2 (Supplementary Information). The highest
464 contents of OC were 11.4, 7.0 and 4.1 µ gm^{-3} for NAR-1, NAR-2 and NPC, respectively. In
465 NPC, OC/EC varied between 0.6 and 4.2, half the values found in NAR.
466 Marked differences were observed for some polyols and sugars between sites and sampling
467 years (Table 1).
468 Levoglucosan reached a maximum monthly concentration of 107 ngm^{-3} in NAR-2 (August
469 2016) and 111 ngm^{-3} in NPC (March 2016). Mannosan and galactosan total mean
470 concentrations ranged from 0.9 to 10 ng m^{-3}.
471 Monthly concentrations of the sum of polyols (Fig. SI-2, Supplementary Information) varied
472 from 9 to 609 and from 6 to 171 ng m^{-3} in the NAR and NPC areas, respectively. Polyols
473 concentrations over the three sampling sites were classified in decreasing order as follows:
474 mannitol>arabitol>sorbitol, with the highest concentrations recorded in NAR.

475

476 **3.4 PACs content of PM_{10}**

477 The sum of oxy-PAHs, nitro-PAHs and PAHs in PM_{10} was four to six times higher in NPC than
478 in NAR. Nitro-PAH concentrations were not significant (under 5 pg m^{-3}) for all the sites.
479 Concentrations of these compounds were higher in NAR-1 than in NAR-2 (Table 1).
480 Among the PAHs: naphtalene, benzo[b]fluoranthene + benzo[j]fluoranthene +
481 benzo[k]fluoranthene, indeno[1,2,3-c,d]pyrene and benzo[g,h,i]perylene reached the highest
482 annual mean concentrations in NPC, varying from 180 to 373 pg m^{-3} (Table SI-6). There are
483 no maximum permissible limits for all of these compounds.
484 In all sampling sites, benzo[a]pyrene concentrations in PM_{10} remained below the maximum
485 annual average permissible level of 1 ng m^{-3} according to the European Union (Table SI-5). As
486 mentioned in the methodology for levoglucosan results, sampling time (one month in the
487 Amazon region) may have led to volatilasation or degradation of these compounds towards
488 secondary species contributing to underestimation. For this reason, we have also analysed the
489 gas phase (Fig. 2).

490

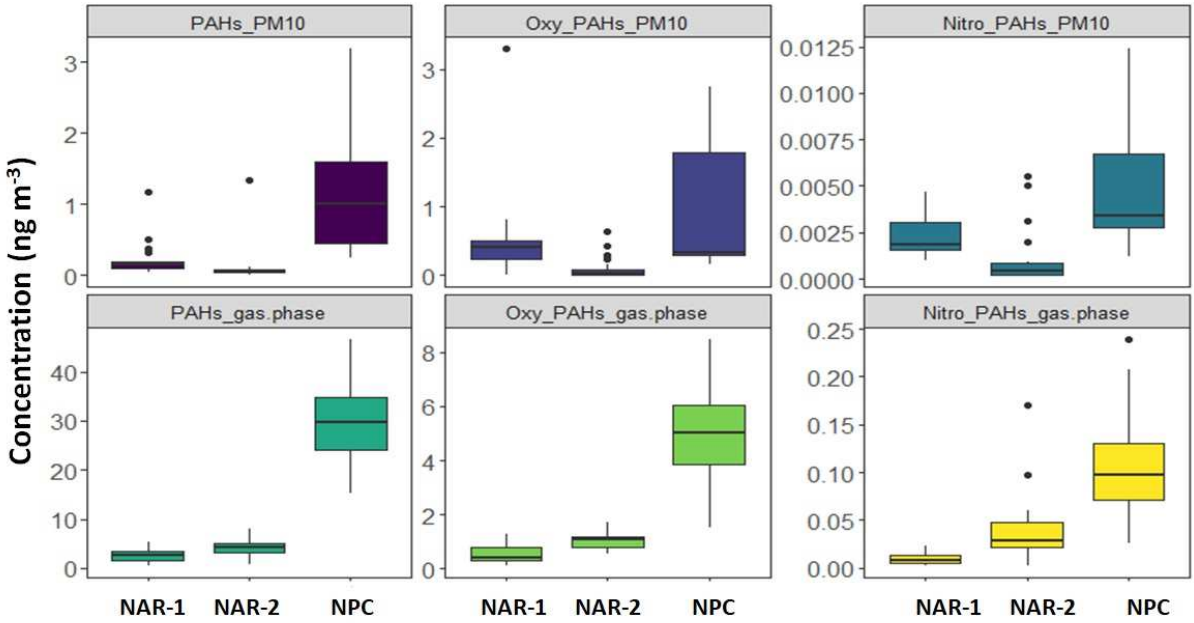

Fig. 2. Mean concentration (ng m^{-3})* of PACs§ in the particulate (PM_{10}) and gas phase (PAHs_gas) from the three sampling sites: NAR-1 (Auca in Orellana) and NAR-2 (Shuara in Sucumbios), both in NAR of Ecuador and NPC (La Florida in Esmeraldas).
**two years of sampling*
§List of PACs is available in Table SI-2 of Supplementary Information.

The gas phase contributes 95, 98 and 97% of the total PAHs, to 46, 94, 95% of the total oxy-PAHs and 80, 91, 97% of the total content of nitro-PAHs in NAR-1, NAR-2 and NPC, respectively. The NPC displayed the highest content in the gas phase with an average of 32 ng m^{-3} for PAH and 7 ng m^{-3} for oxy-PAHs (Table 1).

3.5 OP assays and ROS generation

Results of OP from monthly PM_{10} filters (10 to 12 filters per year for NAR stations and up to 23 for NPC) measured by three different assays are shown in Fig. 3.

Among all sampling sites, NPC presents the highest ROS generation potential for all OP assays, followed by NAR-2 and NAR-1. An increase in OP in 2016 matched an increase of PM_{10} in 2016 at NPC.

For NAR-2, OP^{DCFH} and OP^{DTT} provided similar information, whereas OP^{AA} displayed a noticeable difference between 2015 and 2016.

Annual OP^{DTT} in both NAR locations was below 1.2 nmol DTT min^{-1} m^{-3}, whereas it was three-fold higher in NPC. The OP^{DCFH} exhibited a similar trend in NAR (< 1 nmol [H_2O_2] eq. m^{-3} in NAR-1), being three-fold higher in NPC. The lowest values were measured in NAR-1, with OP^{AA} below 0.5 nmol AA min^{-1} m^{-3}.

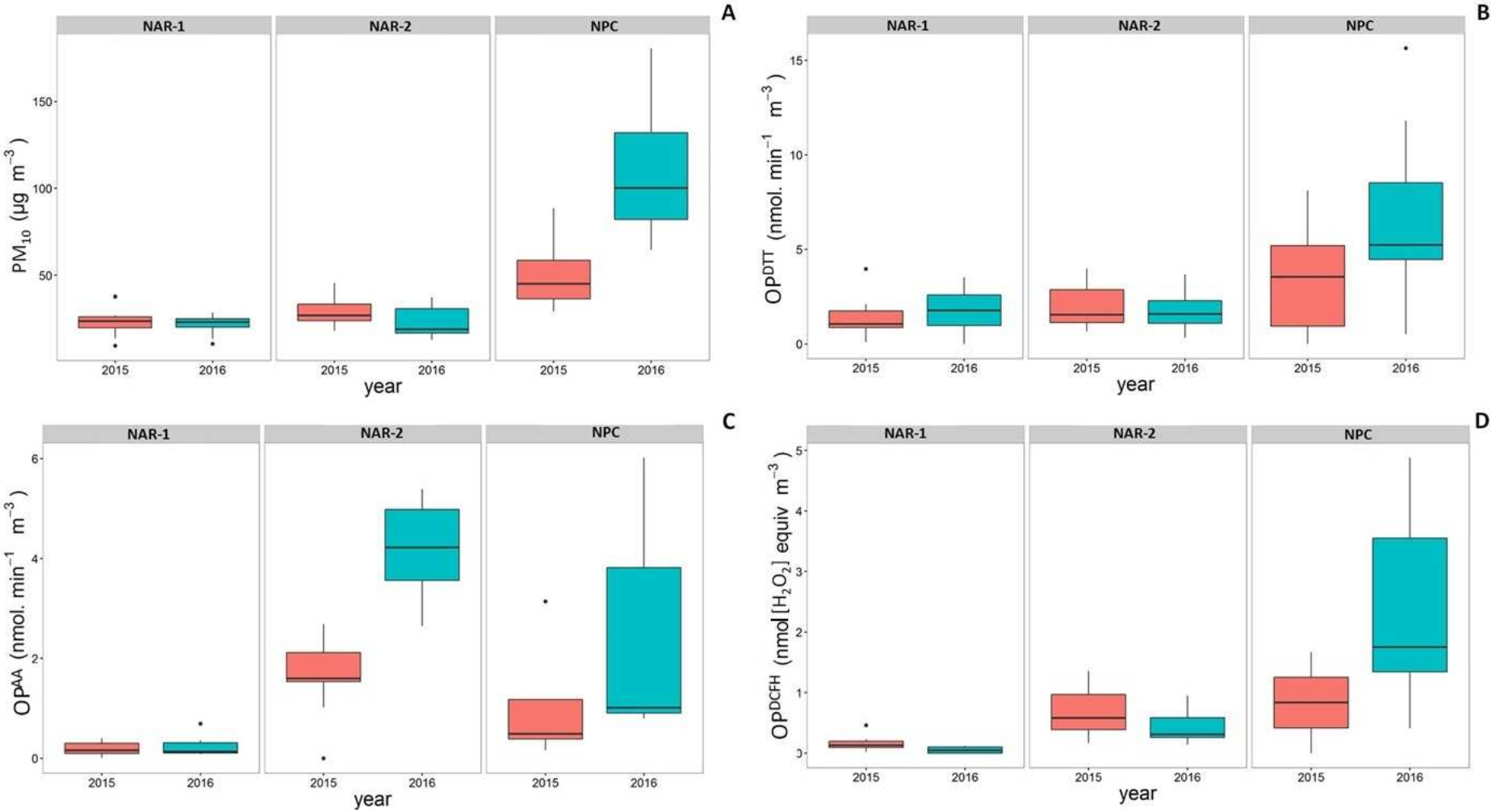

Fig. 3. A) PM_{10} mass concentration (µg m^{-3}) *versus* **B)** oxidative potential (OP, m^{-3}) measured by Dithiothreitol (DTT) assay; **C)** ascorbic acid (AA) assay and **D)** dichlorofluoresceine (DCFH) assay in NAR-1 (Auca in Orellana), NAR-2 (Shuara in Sucumbios), both in NAR and NPC (La Florida in Esmeraldas) for 2015 and 2016.

4. Discussion

4.1 PM_{10} mass reconstruction

Species contribution to PM_{10} mass balance for each site is shown in Fig. 4. Even if NAR-1 and NAR-2 are located in two different provinces, Orellana and Sucumbíos, respectively, both sampling sites display similar mass contributions. Small villages in the NAR of Ecuador appeared as a consequence of the roads opening into the rainforest to establish oil activities (Lessmann et al., 2016). Hence, in rural sites like these, OM rates might be dominated by biogenic emissions from the remaining forest (soils and plants) and by episodes of biomass burning related to agricultural practices or deforestation (Medeiros et al., 2006). In both provinces, the deforestation rates calculated for 2013 ranged from 10 to 15% of the primary forest (RAISG, 2015). Even so, the contribution of OM to the PM_{10} mass in NAR was 32 to 37% and major elements (accounting for 47% PM_{10}) may have originated from soil dust resuspension (Fig. 4).

In contrast, NPC displays a more urban and industrial profile. Esmeraldas is a coastal city with scattered patches of tropical rainforest and dry forest. Oil refining, thermoelectric stations, vehicular traffic and sea salts are the main sources of ambient particles in this area. The OM contribution was 5%, about six times lower than in NAR. Soil elements and sea salts accounted for 40 and 27%, respectively. EC also exhibited higher percentages in NPC than in NAR, i.e., 9% vs 3–5% of total PM_{10} mass (Fig. 4).

Soluble ions accounted for 4.5 and 8% in NPC and NAR, respectively, while trace elements in both areas represented less than 2%.

In NPC, total contribution of SO_4^{2-} (sea salt and non-sea salt) for PM_{10} mass balance was around 8%. Regarding the OM fraction, only 4% of the compounds were identified: ∑(monosaccharide anhydrides, polyols+glucose) and ∑(PAHs + oxy-PAHs + nitro-PAHs) accounted for 90 and 10%, respectively.

In the NAR, between 2 and 3% of the OM compounds were identified with a difference, in that PAHs contributed less than 1% and the rest came from monosaccharides, polyols and sugars. In both areas, the contribution of polyols (from biogenic emissions) to OM was higher than the tracers of biomass burning. Chemical balance closure for NPC and NAR was satisfactory with a range of non-identified compounds within 2 to 14%.

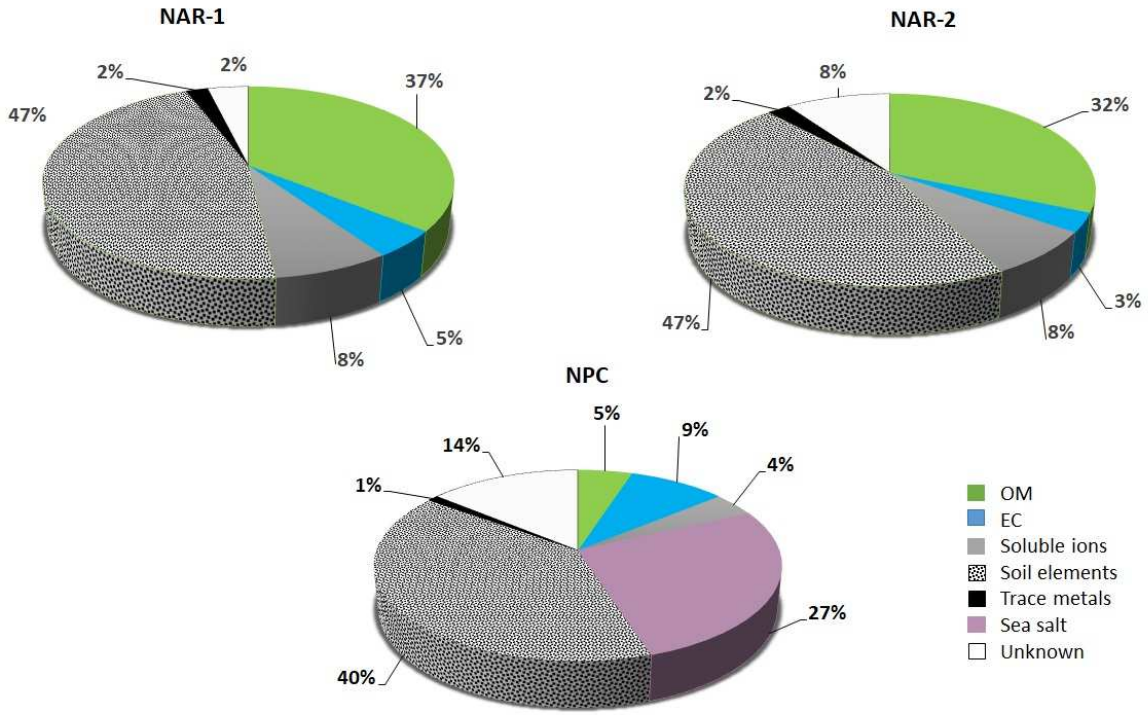

Fig. 4. PM_{10} mass balance for NAR-1 (Auca in Orellana) and NAR-2 (Shuara in Sucumbíos) stations in the Ecuadorian NAR and NPC (La Florida in Esmeraldas).
OM stands for organic matter and EC for elementary carbon.

Waked et al. (2014) showed that in Lens (France), a region with many petrochemical, metallurgic and non-metallurgic industries, OM, EC, SO_4^{2-}, NH_4^+, NO_3^- and other compounds (Cl^-, major and trace elements) accounted for almost 30, 5, 12, 8, 21 and 9% of PM, respectively. In the same study, the non-identified fraction was about 14%, whereas more than 5% of the compounds in the OM were identified: 56% corresponding to levoglucosan, 24% to ∑polyols, 9% to mannosan, 3% to galactosan and 8% to glucose.

It should be noted that several organic compounds that contribute to the OM fraction were not quantified in our study. These compounds include: carboxylic acids, naturally present in plant waxes (Santos et al., 2014); humic-like substances (HULIS) (Graber and Rudich, 2006; Zhao et al., 2016) and volatile organic compounds (VOCs), such as BTEX (benzene, toluene, ethylbenzene and xylene) issued from biogenic and anthropogenic sources (Baltrenas et al., 2011; Zhang et al., 2017).

The remaining mass ("unknown" fraction) could also be assigned to water bound to particles, measurement errors (i.e., weighting samples), volatilization of species due to sampling time and local meteorological conditions or constraints in choosing an appropriate mass balance equation as suggested by Chow et al. (2015) and Malm et al. (2011).

4.2 PM_{10} composition and identification of potential sources

576 Recent literature published data on PM_{10} mass concentrations for two cities in Ecuador (Quito
577 and Cuenca), both located in the Andes mountains, and influenced by industry, thermoelectric
578 stations and traffic. Concentrations ranged from 24 and 77 µg m^{-3} for Quito (Raysoni et al.,
579 2016) and between 32 and 46 µg m^{-3} for Cuenca (Palacios and Espinoza, 2014). Even if these
580 results are not comparable to both regions of our study, PM_{10} concentrations were within such
581 ranges, except for the substantial increase observed in NPC in 2016. This is mainly explained
582 by the downtime, renovation and restart of the oil refinery in Esmeraldas with twice its initial
583 capacity (Table 1 and Fig. SI-1).
584 In the NAR, PM_{10} mass concentrations ranged from 9.39 to 45 µg m^{-3} (Fig. SI-1), with an
585 increase in the wet season, but only in NAR-1. Our results were higher than those found in the
586 Brazilian Western Amazon in Manaus (annual mean of 5 µg m^{-3} in a forest reserve in pristine
587 condition) (Artaxo et al., 2013); similar to those found in Porto Velho by De Oliveira Alves et
588 al. (2015)(13.38 to 30.20 µg m^{-3} depending on season) in an area highly impacted by land use
589 change and biomass burning.
590
591 Regarding elements associated with soil dust, Artaxo et al. (2013) found that concentrations
592 of Al, Ca, Fe, Si and Ti in Manaus were less than 300 ng m^{-3}, supported by the fact that soil
593 was covered by plant debris, reducing natural emissions and resuspension. By contrast, in
594 Porto Velho these concentrations were about eight times higher, but still lower than those
595 recorded in the Ecuadorian NAR (Table 1).
596 Gilardoni et al. (2011) reported that trace elements (Cr, Cu, Ni, Pb, V, Ti, Sb and Zn) in Porto
597 Velho (pristine rainforest) in the coarse fraction were 8 to 28 times lower than the
598 concentrations reported in our study (except for Pb and Sb which are in the same range) (Table
599 1). All these findings may suggest that anthropogenic activities in NAR greatly affect the air
600 quality in comparison to pristine Amazon forests in Brazil.
601
602 Trace elements such as Ba, Mo, Ni and V have been reported as air pollutants commonly
603 emitted during oil refining operations (Islam et al., 2010), whereas Ni and V are proxies for the
604 combustion of heavy oil being ubiquituos for shipping emissions and petroleum industry
605 (Moreno et al., 2010). Ni and V displayed higher concentrations in NAR than in Quito, but in
606 $PM_{2.5}$ (Raysoni et al., 2017). Similar contents of Ni and V in NPC (Table 1) were found in La
607 Linea/Algeciras, the main shipping area and petrochemical complex of Spain (Moreno et al.,
608 2010). As a rough comparison (assuming that the chemical composition of PM_{10} and $PM_{2.5}$
609 differs), Ba and Mo in NAR and in NPC reached concentrations from 2 to 7 and from 200 to
610 1000 times higher than those reported by Raysoni et al.(2017) for $PM_{2.5}$ in Quito.
611

612 Literature is scarce about Mo in the air, but concentrations between 10 and 30 ng m^{-3} are
613 commonly reported in urban areas and between 1 and 3.2 ng m^{-3} in rural areas (ATSDR, 2017).
614 This is in disagreement with our study because the mean Mo concentration in NAR and NPC
615 reached 47.5 and 126 mg m^{-3}, respectively, by far higher than those reported in the US or
616 Europe (Alleman et al., 2010; Fernández-Olmo et al., 2016; Hama et al., 2018). Molybdenum
617 is used as a catalyzer during refining of heavy crude oil (Mironenko et al., 2017; Pradhan et
618 al., 2013), as a friction reduction additive (Humood et al., 2019) and as a weighting agent in
619 drilling fluids (McDaniel and Jamison, 2014). Concentrations of Mo in PM_{10} collected in a
620 heavily industrialized site located adjacent to one of the largest petrochemical complexes in
621 the US and related to the combustion of crude oil (in association with Ni, V and Sc)(Bozlaker
622 et al., 2013) were 73 to 1000 times lower than the concentrations measured in NPC.
623 Similar results occur with Ba. Despite it not being regulated, its concentration in the air should
624 remain below 8 ng m^{-3} (ATSDR, 2007). Even if Ba in PM_{10} originates from crustal dust, it is
625 commonly used as a weighting agent in drilling fluids (Do Amaral Sobrinho et al., 2018;
626 Oskarsson, 2015). The PM_{10} collected between the Mediterranean and Atlantic coasts showed
627 daily concentrations of Ba varying from 0.8 to 49.1 ng m^{-3}, associated with crustal and
628 anthropogenic sources such as shipping fuel and oil combustion (Moreno et al., 2010).
629 Therefore, high Ba, Mo, V and Ni concentrations may evidence the impact of oil extraction and
630 refining on the atmospheric composition in both regions. These four elements can be
631 considered as specific tracers of oil activities in the Ecuadorian environment.
632
633 Total mean cation concentrations in NAR (Table 1) were double compared to those reported
634 by Gilardoni et al. (2011)—20 to 80 ng m^{-3} in the coarse mode—in a pristine rainforest located
635 in northern Manaus, where they were mainly associated with biogenic emissions.
636 Yamasoe et al. (2000) found SO_4^{2-} to be the most important inorganic ion in biomass burning
637 aerosols in Amazonia. Its percentage varied as a function of the burning phase, smoldering
638 *versus* flaming, reaching mean values of 0.35–0.72% and 0.39–0.90% of the PM_{10} mass,
639 respectively.
640 In the Ecuadorian Amazon, sulfate concentrations represent between 3 and 5% of the total
641 PM_{10} mass in NAR-2 and NAR-1, respectively, suggesting that other sources might contribute
642 to SO_4^{2-} contents. Likewise, chemical analyses of rain and fog water samples collected in the
643 mountainous rain forest of southern Ecuador showed frequent episodes of high sulfate and
644 nitrate emissions, assigned to biomass burning from areas upwind of the Amazon basin
645 (Fabian et al., 2005). Sulphates can also be secondary products from oil and gas extraction
646 procedures (Sarnela et al., 2015; Tuccella et al., 2017).
647 Sulphate is also a prevalent tracer of sea salt sources that should be considered in the NPC
648 area. In this site, SO_4^{2-} reached annual mean concentrations of 2556 and 3120 ng m^{-3} in 2015

649 and 2016, respectively (Table 1), evidencing both industrial and seawater emissions. These
650 values were within the range of concentrations found in coastal industrial cities in Europe like
651 Barcelona, Porto and Athens, which also have petrochemical plants (Amato et al., 2016).
652 Moreover, Ecuadorian oil is known to contain high-sulfate contents, between 0.99±0.08 and
653 1.34±0.27% (samples collected from the National Oleoduct and an oil camp) that may also
654 explain a part of the sulfate fraction.
655
656 Among organic compounds, levoglucosan (main pyrolysis product from cellulose), galactosan
657 and mannosan (derived from hemicellulose) lead to tracers for biomass burning episodes with
658 concentrations that vary depending on region and season (Chen et al., 2017; Cheng et al.,
659 2013; Li et al., 2017). As a general trend, concentrations of these compounds in NAR and
660 NPC, were much lower in comparison to the literature about wood burning and deforestation
661 in the Amazonian region (De Oliveira Alves et al., 2015), suggesting that the Amazon region
662 in Ecuador is nowadays less impacted by land use change and biomass burning.
663 On the other hand, total mean concentrations of levoglucosan, mannosan and galactosan in
664 NPC were within the range of those in Barcelona obtained by Reche et al. (2012), but in $PM_{2.5}$
665 as related to agricultural waste burning and long-distance transport of aerosols from forest
666 fires. However, the levoglucosan concentration in NPC was four times lower than those
667 recorded by Oliveira et al. (2007) in the coarse fraction in Oporto (Portugal) and probably
668 originated from wood burning ovens and fireplaces. Thus, the NPC area could be impacted by
669 similar sources.
670 Ratios of 11 to 18 for OC/EC recorded in Porto Velho by De Oliveira Alves et al. (2015) were
671 two to three times higher than those calculated for NAR (Table 1, Fig. SI-2). This suggests that
672 biomass burning is of a lesser impact in our rural sampling sites and probably related to
673 limitations in our methodology (section 2.3.4).
674 Esmeraldas (NPC sampling site) with over 500 000 inhabitants, showed OC/EC ratios similar
675 to those found in urban and industrial site profiles similar to sites in Spain and Portugal, ranging
676 from 1.8±0.8 to 2.8±1.3 (Oliveira et al., 2007; Reche et al., 2012).
677
678 In regards to organic compounds, PAH concentrations were different between the two
679 sampling sites located in NAR (Table 1, Fig. 2). Since air samplers at both sites were located
680 an equal distance from open flares and similar PM_{10} concentrations were observed, differences
681 in PAH content could be due to the size of open flares (bigger in NAR-1), to the number of
682 flares (one in NAR-1, four in NAR-2) and to the close environment (wooded area in NAR-1).
683 Total PAH (PM+gas phase) concentrations in NAR were two to five times higher than oxy-
684 PAHs, while nitro-PAHs were 90 to 224-fold lower. Similarly, French sites such as Marseille

(shipping+oil activities) or alpine valleys display the same order of magnitude for PAHs and oxy-PAHs (Albinet et al., 2008, 2007).

Total PAHs (PM+gas phase) in NPC (Table 1, Fig. 2) were on the order of magnitude of concentrations recorded in Porto (30 ng m^{-3} in a shipping and oil activities areas) (Albuquerque et al., 2016) or in the Amazonian forest in Brazil (35 ng m^{-3}) as reported by Krauss et al., (2005).

Concentrations of 0.13±0.04 ng m^{-3} and 6.54±0.88 ng m^{-3} in NPC for nitro-PAHs and oxy-PAHs, respectively (PM_{10}+gas phase), are in the lowest range of the main French shipping and oil activities area of Marseille or Athens, Greece (Albinet et al., 2007; Andreou and Rapsomanikis, 2009). Conversely, in NAR, values of total nitro-PAHs in the range of 0.01 to 0 0.05 ng m^{-3} was low as observed in rural sites in North China (0.013–3.70 ng m^{-3}) or in a remote area of Chile (0.001 ng m^{-3})(Li et al., 2015; Scipioni et al., 2012).

In the particulate phase, nitro-PAHs ranged between 1–5 pg m^{-3} for the three sampling sites and must be considered in the lowest range of available literature: 9–19 pg m^{-3} in Paris in summer (Ringuet et al., 2012) and 18–1546 pg m^{-3} in Sao Paulo in summer (De Castro Vasconcellos et al., 2008).

Thus, the low concentrations recorded for particulate PAHs can be explained by volatilization due to high temperatures and an extended sampling period (as well as for levoglucosan, see section 2.2).

4.3 Identification of PM_{10} chemical components generating ROS

Saffari et al. (2014) reported OP^{DTT} between 1.4 nmol min^{-1} m^{-3} for urban background up to 3.3 nmol min^{-1} m^{-3} for a highway traffic place. Total mean values for OP^{DTT} over a two-year sampling period were two-fold higher in NPC (Fig. 3), displaying an important oxidative burden. Conversely, in the NAR, total mean OP^{DTT} varied between 1.63 and 1.83 nmol min^{-1} m^{-3}.

Concerning the DCFH assay, Hedayat et al. (2015) reported DCFH oxidation rates up to 3.81 nmol [H_2O_2] eq. m^{-3} for urban sites which are in agreement with NPC values (Fig. 3). As observed for OP^{DTT}, OP^{DCFH} remained lower for both NAR sites.

In spite of almost equivalent PM_{10} mass concentrations for the two-year sampling period in NAR-1 and NAR-2, OP^{AA} was different between 2015 and 2016. OP^{AA} is known to be highly sensitive to metals (Hedayat et al., 2015; Szigeti et al., 2015). Being the concentration of trace elements was higher in NAR-2 than in NAR-1, it is not surprising that OP values reached higher values at the former site. However, this increase of OP^{AA} in 2016 at NAR-2 is not totally understood considering that PM_{10} and its composition were stable over 2015-2016.

Taken together, these three complementary OP assays highlight the importance of ROS exposure for NPC residents, a polluted and industrial site as compared to an acceptable exposure in the rural or urban background in NAR.

Several studies have already indicated that ROS formation as measured by OP assays is strongly driven by PM reactivity and redox compounds (Calas et al., 2018; Charrier et al., 2015; Eiguren-Fernandez et al., 2010; Yang et al., 2014). To determine which particulate compounds were responsible for ROS formation in NAR and NPC, a correlation matrix according to Spearman's test (chosen because of the non-normal data distribution) was calculated (Fig. 5). In the oil extraction area, OP^{DTT} was correlated with Ba, Ni, NH_4^+, Si and Zn (r ~0.8); moderately with OC, TC and polyols (r ~0.5); and had a negative correlation with benzanthrone, fluoranthene and perylene (r_s> -0.8). OP^{AA} was strongly correlated to EC, mannosan and galactosan (r_s 0.7–0.8) and inversely correlated with Al, Co and Zn (r_s> -0.7) in NAR-1. In NAR-2, OP^{DCFH} was either low or not positively correlated to any of the investigated chemical compounds; the same for OP^{DTT}.

However, OP^{AA} was strongly correlated (r_s> 0.8) with Ba, moderately correlated with some oxy-PAHs (i.e., napthtoquinone) and PAHs (i.e., BaP) and polyols, and inversely correlated with Al, Cr, $NO_3^-$and Sn. OP^{DCFH} was not correlated with any compound.

In the oil refining area (NPC), OP^{DTT} was moderately correlated with As, Ba, Ni, Zn and NH_4^+ and inversely correlated with Cl^-, Ca^{2+} and ∑oxy-PAHs. OP^{AA} was strongly correlated with Ba and NH_4^+ (r_s> 0.7), but inversely to metals (Co, Cr, Fe, Sn). Finally, OP^{DCFH} was moderately correlated to MSA, NH_4^+, Ba, Ni and Zn and strongly correlated to levoglucosan, MSA and NH_4^+.

Our results showed that OP^{AA} and OP^{DCFH} were correlated with Ba (oil tracer) for all sites. Perrone et al. (2013) reported that Ba in $PM_{2.5}$ and PM_1 may induce cytotoxicity in human alveolar cells. It has been reported that exposure to Ba can produce oxidative stress in mammals and impair cellular antioxidant defense systems like glutathione (Elwej et al., 2017).

Nevertheless, there is not conclusive information about Ba redox activity in lung cells, but it is probable that its emission during oil activities is bound to other compounds that are redox active.

Despite high concentrations of Mo in PM_{10}, this element shows a low to moderate correlation with OP results. In contrast, Ni and V were moderately to strongly correlated with OP assays in NPC as they are supposed to be tracers of shipping traffic and oils activities (Pey et al., 2013). It has been observed that both elements are able to generate hydroxyl radicals when they come into contact with biological cells (Verma et al., 2009).

PAHs can induce oxidative stress indirectly if they are oxidized to polar compounds including quinones and possibly nitro-PAHs, which are redox active compounds (Cho et al., 2005; Li et al., 2002; Squadrito et al., 2001). OP assays were strongly correlated with some individual oxy-PAHs or nitro-PAHs compounds (e. g. 1,4 napthoquinone; 9, 10 antraquinone, benzenthrone with $r > 0.7$ in NAR-2; 9, 10 antraquinone with $r > 0.8$ in NPC).
Polyols were moderately correlated with ROS generation in both NAR sites where biogenic emissions are prevalent and recently shown to contribute to OP values (Samaké et al., 2017).

Such correlations provide interesting information about sources of emission possibly involved in ROS exposure from PM: (i) in NAR-1, OP^{DTT} is mainly correlated with oil extraction tracers and anthropogenic emissions from biomass burning; (ii) in NAR-2, OP^{AA} is associated with oil extraction proxies (Ba and oxy-PAHs) and (iii) in NPC, OP^{AA} and OP^{DCFH} assays agree in pointing to oil refining and thermoelectric industrial tracers (Ni, Ba), and possibly road traffic.

Finally, these results indicate that the population living in the vicinity of the Esmeraldas National Oil Refinery and the Thermoelectric plant (in NPC) has a significant exposure to ROS and are potentially impacted by oxidative stress due to PM inhalation more than those living in the oil extraction area of the Amazonian region (NAR).
All these trends must be confirmed by a source apportionment to assign PM emission sources to their overall ROS contribution (Weber et al., 2018), but that would involve a more intensive sampling that would be difficult to maintain under the sampling conditions described in section .

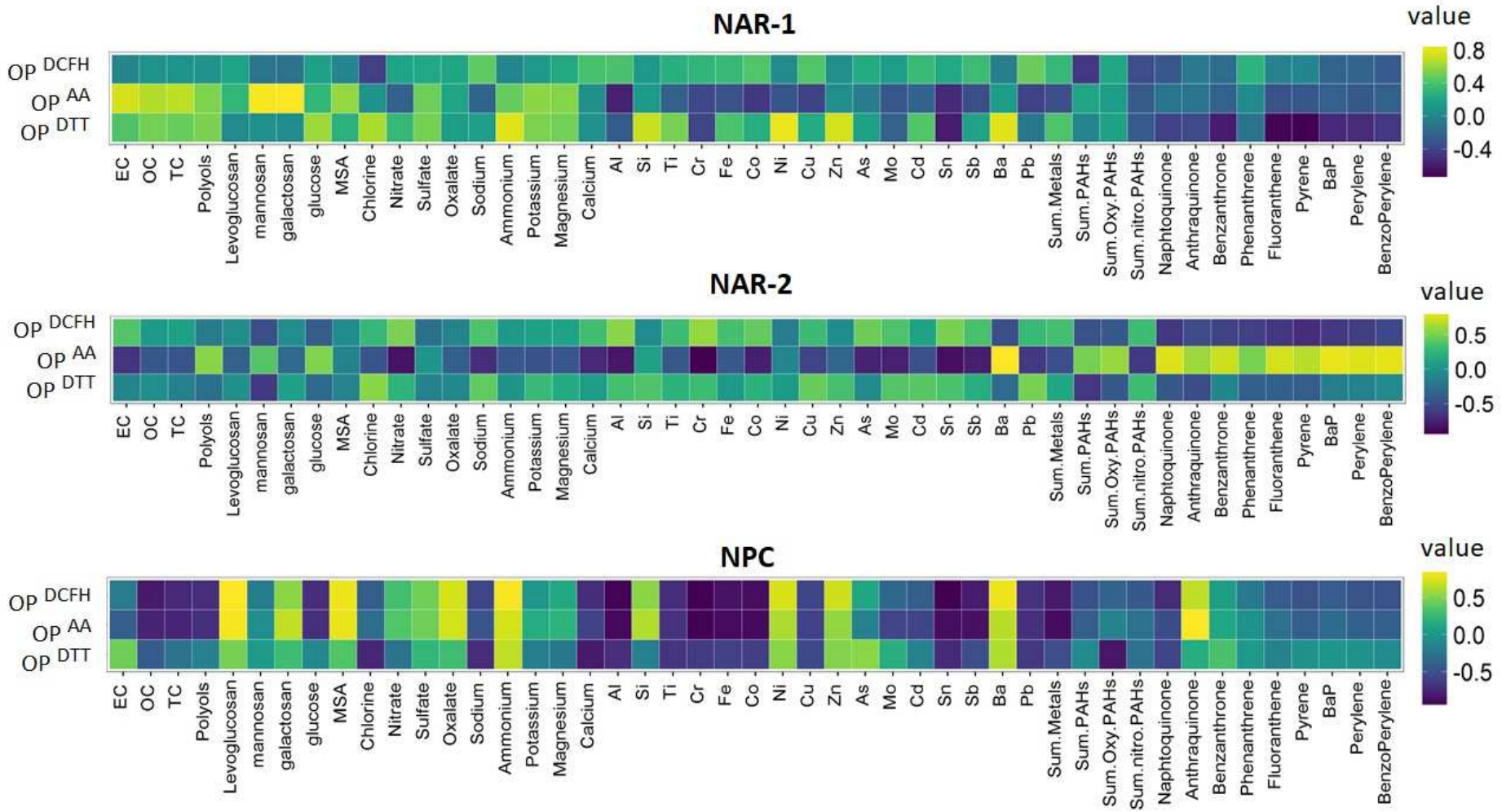

779

780 **Fig. 5.** Correlation matrix according to Spearman's coefficient for a subset of chemical species determined in PM_{10} and the three OP assays for
781 NAR-1 (Auca in Orellana), NAR-2 (Shuara in Sucumbíos) and NPC (La Florida in Esmeraldas) sampling stations.

5. Conclusions

The chemical composition of PM_{10} in oil producing and refining areas in Ecuador not only depends on the type of oil activity but also on other anthropogenic sources as well as on the natural environment. Even if no seasonality was evidenced in NAR-2, more pronounced variations with time and between sampling years have been observed for some compounds, especially for sugars and PAHs, mainly in NPC and probably due to the shutdown and rehabilitation of the refinery in 2015.

In the NAR area, OM and soil elements were the dominant fractions of PM_{10} composition, indicating that biogenic and soil dust emissions are the main sources of atmospheric particles. By contrast, in NPC, sea salts and soil elements were the major compounds. Contribution of EC to the PM_{10} mass balance in the NPC area was significant, highlighting industrial emissions due to oil refining processes. PAHs also contributed to a higher percentage of OM in NPC (10%) than in NAR (less than 2%). Trace elements like Ba and Mo, both widely used in oil production and refining, and not usually reported in studies on air quality, showed higher concentrations than those recorded in urban-industrialized sites in Quito, US or Europe. Thus, Ba, Mo, Ni and V can be considered as relevant tracers of oil activities in Ecuador.

ROS formation depends on the airborne chemical composition and was specific to each region. The PM from NPC exhibited a very high ROS generation capacity, representative of industrials sites, whereas PM from both NAR stations presented an overall OP attributed to rural sites. Additionally, OP assays in combination with PM detailed composition evidenced that oil activities in combination with biogenic emissions in NAR and with other industrial emissions in NPC, are responsible for the PM capacity for ROS generation. Finally, this study reported that elevated concentrations of PM chemical constituents previously associated with adverse human health (Barraza et al., 2018) were identified at the three sampling sites. The present study opens the way for further investigations in epidemiology and risk assessment in the areas presented here, but also in other Latin America and African countries where oil activities are widely developed without relevant environmental and health policies.

Acknowledgments:

The authors would like to thank the French National Research Agency for the financial support of the ANR-MONOIL Project N°ANR-13-SENV-0003-01. The IGE institute is member of the Cluster of Excellence (LabEx) OSUG@2020 (ANR-10-LABX-56) and the LPTC team from EPOC is member of the LabEx COTE (ANR-10-LABX-45). We want to thank the National Program of Innovation for the Competitiveness and Productivity of Peru, for the PhD grant N°139-Innóvate Perú-BDE-2014 of the first author. We want to express our gratitude to the Ramirez and Garcia families in Ecuador for their special care on filter's removal, and to

Petroecuador National Oil Company for their technical support in Esmeraldas. Finally, we are very grateful to Mathieu Boidot for statistical advises and R graphical representations.

References

Agency for Toxic Substances and Disease Registry (ATSDR), 2017. Toxicological profile for Molybdenum (Draft for Public Comment). U.S. Department of Health and Human Services, Public Health Service.

Agency for Toxic Substances and Disease Registry (ATSDR). Toxicological profile for Barium. Atlanta, GA: U.S. Department of Health and Human Services, Public Health Service.

Albinet, A., Leoz-Garziandia, E., Budzinski, H., Villenave, E., 2007. Polycyclic aromatic hydrocarbons (PAHs), nitrated PAHs and oxygenated PAHs in ambient air of the Marseilles area (South of France): concentrations and sources. Sci. Total Environ. 384, 280–292. https://doi.org/10.1016/j.scitotenv.2007.04.028

Albinet, A., Leoz-Garziandia, E., Budzinski, H., Villenave, E., 2006. Simultaneous analysis of oxygenated and nitrated polycyclic aromatic hydrocarbons on standard reference material 1649a (urban dust) and on natural ambient air samples by gas chromatography–mass spectrometry with negative ion chemical ionisation. J. Chromatogr. A 1121, 106–113. https://doi.org/10.1016/j.chroma.2006.04.043

Albinet, A., Leoz-Garziandia, E., Budzinski, H., Villenave, E., Jaffrezo, J.-L., 2008. Nitrated and oxygenated derivatives of polycyclic aromatic hydrocarbons in the ambient air of two French alpine valleys. Part 1: Concentrations, sources and gas/particle partitioning. Atmos. Environ. 42, 43–54. https://doi.org/10.1016/j.atmosenv.2007.10.009

Albuquerque, M., Coutinho, M., Borrego, C., 2016. Long-term monitoring and seasonal analysis of polycyclic aromatic hydrocarbons (PAHs) measured over a decade in the ambient air of Porto, Portugal. Sci. Total Environ. 543, 439–448. https://doi.org/10.1016/j.scitotenv.2015.11.064

Alleman, L.Y., Lamaison, L., Perdrix, E., Robache, A., Galloo, J.-C., 2010. PM10 metal concentrations and source identification using positive matrix factorization and wind sectoring in a French industrial zone. Atmospheric Res. 96, 612–625. https://doi.org/10.1016/j.atmosres.2010.02.008

Amato, F., Alastuey, A., Karanasiou, A., Lucarelli, F., Nava, S., Calzolai, G., Severi, M., Becagli, S., Gianelle, V.L., Colombi, C., Alves, C., Custódio, D., Nunes, T., Cerqueira, M., Pio, C., Eleftheriadis, K., Diapouli, E., Reche, C., Minguillón, M.C., Manousakas, M.-I., Maggos, T., Vratolis, S., Harrison, R.M., Querol, X., 2016. AIRUSE-LIFE+: a harmonized PM speciation and source apportionment in five southern European cities. Atmospheric Chem. Phys. 16, 3289–3309. https://doi.org/10.5194/acp-16-3289-2016

Andreou, G., Rapsomanikis, S., 2009. Polycyclic aromatic hydrocarbons and their oxygenated derivatives in the urban atmosphere of Athens. J. Hazard. Mater. 172, 363–373. https://doi.org/10.1016/j.jhazmat.2009.07.023

Artaxo, P., Rizzo, L.V., Brito, J.F., Barbosa, H.M.J., Arana, A., Sena, E.T., Cirino, G.G., Bastos, W., Martin, S.T., Andreae, M.O., 2013. Atmospheric aerosols in Amazonia and land use change: from natural biogenic to biomass burning conditions. Faraday Discuss. 165, 203. https://doi.org/10.1039/c3fd00052d

Avdalović, J., Đurić, A., Miletić, S., Ilić, M., Milić, J., Vrvić, M.M., 2016. Treatment of a mud pit by bioremediation. Waste Manag. Res. 34, 734–739. https://doi.org/10.1177/0734242X16652961

Baklanov, A., Molina, L.T., Gauss, M., 2016. Megacities, air quality and climate. Atmos. Environ. 126, 235–249. https://doi.org/10.1016/j.atmosenv.2015.11.059

Baldasano, J., Valera, E., Jimenez, P., 2003. Air quality data from large cities. Sci. Total Environ. 307, 141–165. https://doi.org/10.1016/S0048-9697(02)00537-5

Baltrenas, P., Baltrenaite, E., Sereviciene, V., Pereira, P., 2011. Atmospheric BTEX concentrations in the vicinity of the crude oil refinery of the Baltic region. Environ. Monit. Assess. 182, 115–127. https://doi.org/10.1007/s10661-010-1862-0

Barraza, F., Maurice, L., Uzu, G., Becerra, S., López, F., Ochoa-Herrera, V., Ruales, J., Schreck, E., 2018. Distribution, contents and health risk assessment of metal(loid)s in small-scale farms in the Ecuadorian Amazon: An insight into impacts of oil activities. Sci. Total Environ. 622–623, 106–120. https://doi.org/10.1016/j.scitotenv.2017.11.246

Boisa, N., Elom, N., Dean, J.R., Deary, M.E., Bird, G., Entwistle, J.A., 2014. Development and application of an inhalation bioaccessibility method (IBM) for lead in the PM10 size fraction of soil. Environ. Int. 70, 132–142. https://doi.org/10.1016/j.envint.2014.05.021

Borm, P.J.A., Kelly, F., Kunzli, N., Schins, R.P.F., Donaldson, K., 2006. Oxidant generation by particulate matter: from biologically effective dose to a promising, novel metric. Occup. Environ. Med. 64, 73–74. https://doi.org/10.1136/oem.2006.029090

Bourdrel, T., Bind, M.-A., Béjot, Y., Morel, O., Argacha, J.-F., 2017. Cardiovascular effects of air pollution. Arch. Cardiovasc. Dis. https://doi.org/10.1016/j.acvd.2017.05.003

Boy, J., Rollenbeck, R., Valarezo, C., Wilcke, W., 2008. Amazonian biomass burning-derived acid and nutrient deposition in the north Andean montane forest of Ecuador. Glob. Biogeochem. Cycles 22, 1–16. https://doi.org/10.1029/2007GB003158

Boyd, D.R., 2006. The Air we Breathe, an International Comparison of Air Quality Standards and Guidelines, A report prepared for the David Suzuki Foundation. David Suzuki Foundation.

Bozlaker, A., Buzcu-Güven, B., Fraser, M.P., Chellam, S., 2013. Insights into PM10 sources in Houston, Texas: Role of petroleum refineries in enriching lanthanoid metals during episodic emission events. Atmos. Environ. 69, 109–117. https://doi.org/10.1016/j.atmosenv.2012.11.068

Buccina, S., Chene, D., Gramlich, J., 2013. Accounting for the environmental impacts of Texaco's operations in Ecuador: Chevron's contingent environmental liability disclosures. Account. Forum 37, 110–123. https://doi.org/10.1016/j.accfor.2013.04.003

Calas, A., Uzu, G., Kelly, F.J., Houdier, S., Martins, J.M.F., Thomas, F., Molton, F., Charron, A., Dunster, C., Oliete, A., Jacob, V., Besombes, J.-L., Chevrier, F., Jaffrezo, J.-L., 2018. Comparison between five acellular oxidative potential measurement assays performed with detailed chemistry on PM10 samples from the city of Chamonix (France). Atmospheric Chem. Phys. 18, 7863–7875. https://doi.org/10.5194/acp-18-7863-2018

Calas, A., Uzu, G., Martins, J.M.F., Voisin, D., Spadini, L., Lacroix, T., Jaffrezo, J.-L., 2017. The importance of simulated lung fluid (SLF) extractions for a more relevant evaluation of the oxidative potential of particulate matter. Nat. Sci. Rep.7,11617. https://10.1038/s41598-017-11979-3

Charrier, J.G., Anastasio, C., 2012. On dithiothreitol (DTT) as a measure of oxidative potential for ambient particles: evidence for the importance of soluble transition metals. Atmospheric Chem. Phys. Discuss. 12, 11317–11350. https://doi.org/10.5194/acpd-12-11317-2012

Charrier, J.G., Richards-Henderson, N.K., Bein, K.J., McFall, A.S., Wexler, A.S., Anastasio, C., 2015. Oxidant production from source-oriented particulate matter. Part 1: Oxidative potential using the dithiothreitol (DTT) assay. Atmospheric Chem. Phys. 15, 2327–2340. https://doi.org/10.5194/acp-15-2327-2015

Chen, J., Li, C., Ristovski, Z., Milic, A., Gu, Y., Islam, M.S., Wang, S., Hao, J., Zhang, H., He, C., Guo, H., Fu, H., Miljevic, B., Morawska, L., Thai, P., Lam, Y.F., Pereira, G., Ding, A., Huang, X., Dumka, U.C., 2017. A review of biomass burning: Emissions and impacts on air quality, health and climate in China. Sci. Total Environ. 579, 1000–1034. https://doi.org/10.1016/j.scitotenv.2016.11.025

Cheng, Y., Engling, G., He, K.-B., Duan, F.-K., Ma, Y.-L., Du, Z.-Y., Liu, J.-M., Zheng, M., Weber, R.J., 2013. Biomass burning contribution to Beijing aerosol. Atmospheric Chem. Phys. 13, 7765–7781. https://doi.org/10.5194/acp-13-7765-2013

Cho, A.K., Sioutas, C., Miguel, A.H., Kumagai, Y., Schmitz, D.A., Singh, M., Eiguren-Fernandez, A., Froines, J.R., 2005. Redox activity of airborne particulate matter at different sites in the Los Angeles Basin. Environ. Res. 99, 40–47. https://doi.org/10.1016/j.envres.2005.01.003

924 Chow, J.C., Lowenthal, D.H., Chen, L.-W.A., Wang, X., Watson, J.G., 2015. Mass
925 reconstruction methods for PM2.5: a review. Air Qual. Atmosphere Health 8, 243–263.
926 https://doi.org/10.1007/s11869-015-0338-3
927 Crobeddu, B., Aragao-Santiago, L., Bui, L.-C., Boland, S., Baeza Squiban, A., 2017. Oxidative
928 potential of particulate matter 2.5 as predictive indicator of cellular stress. Environ.
929 Pollut. 230, 125–133. https://doi.org/10.1016/j.envpol.2017.06.051
930 Dai, Q., Bi, X., Liu, B., Li, L., Ding, J., Song, W., Bi, S., Schulze, B.C., Song, C., Wu, J., Zhang,
931 Y., Feng, Y., Hopke, P.K., 2018. Chemical nature of PM2.5 and PM10 in Xi'an, China:
932 Insights into primary emissions and secondary particle formation. Environ. Pollut. 240,
933 155–166. https://doi.org/10.1016/j.envpol.2018.04.111
934 De Castro Vasconcellos, P., Sanchez-Ccoyllo, O., Catia Balducci, Mabilia, R., Cecinato, A.,
935 2008. Occurrence and Concentration levels of nitro-PAH in the air of three brazilian
936 cities experiencing different emission impacts. Water. Air. Soil Pollut. 190, 87–94.
937 https://doi.org/10.1007/s11270-007-9582-y
938 De Oliveira Alves, N., Brito, J., Caumo, S., Arana, A., de Souza Hacon, S., Artaxo, P., Hillamo,
939 R., Teinilä, K., Batistuzzo de Medeiros, S.R., de Castro Vasconcellos, P., 2015.
940 Biomass burning in the Amazon region: Aerosol source apportionment and associated
941 health risk assessment. Atmos. Environ. 120, 277–285.
942 https://doi.org/10.1016/j.atmosenv.2015.08.059
943 Do Amaral Sobrinho, N.M.B., Ceddia, M.B., Zonta, E., Magalhães, M.O.L., de Freitas, F.C.,
944 Lima, E.S.A., 2018. Spatial variability and solubility of barium in a petroleum well-drilling
945 waste disposal area. Environ. Monit. Assess. 190. https://doi.org/10.1007/s10661-018-
946 6566-x
947 Ecuador Oil Production 2016. Trading Econ.
948 http://www.tradingeconomics.com/ecuador/crude-oil-production
949 Eiguren-Fernandez, A., Shinyashiki, M., Schmitz, D.A., DiStefano, E., Hinds, W., Kumagai, Y.,
950 Cho, A.K., Froines, J.R., 2010. Redox and electrophilic properties of vapor- and
951 particle-phase components of ambient aerosols. Environ. Res. 110, 207–212.
952 https://doi.org/10.1016/j.envres.2010.01.009
953 Elwej, A., Chaabane, M., Ghorbel, I., Chelly, S., Boudawara, T., Zeghal, N., 2017. Effects of
954 barium graded doses on redox status, membrane bound ATPases and
955 histomorphological aspect of the liver in adult rats. Toxicol. Mech. Methods 1–10.
956 https://doi.org/10.1080/15376516.2017.1351016
957 Empresa Publica Hidrocarburos del Ecuador (EP PetroEcuador), 2013. Monitoreo de calidad
958 del aire en el área de influencia de la Refinería Esmeraldas (Resumen del Monitoreo
959 desde enero 2012 hasta enero 2013). Laboratorio Ambigest. (No. SGER 20111110).
960 EP PetroEcuador.
961 Environmental Performance Index (EPI). Global Metrics for the Environment: The
962 Environmental Performance Index Ranks Countries Performance on High-priority
963 Environmental Issues. http://environment.yale.edu/news/article/2016-yale-
964 environmental-performance-index-released/
965 Fabian, P., Kohlpaintner, M., Rollenbeck, R., 2005. Biomass burning in the Amazon-fertilizer
966 for the mountainous rain forest in Ecuador. Environ. Sci. Pollut. Res. Int. 12, 290–296.
967 Fawole, O.G., Cai, X.-M., MacKenzie, A.R., 2016. Gas flaring and resultant air pollution: A
968 review focusing on black carbon. Environ. Pollut. 216, 182–197.
969 https://doi.org/10.1016/j.envpol.2016.05.075
970 Fernández-Olmo, I., Andecochea, C., Ruiz, S., Fernández-Ferreras, J.A., Irabien, A., 2016.
971 Local source identification of trace metals in urban/industrial mixed land-use areas with
972 daily PM10 limit value exceedances. Atmospheric Res. 171, 92–106.
973 https://doi.org/10.1016/j.atmosres.2015.12.010
974 Foucaud, L., Wilson, M.R., Brown, D.M., Stone, V., 2007. Measurement of reactive species
975 production by nanoparticles prepared in biologically relevant media. Toxicol. Lett. 174,
976 1–9. https://doi.org/10.1016/j.toxlet.2007.08.001
977 Fröhlich-Nowoisky, J., Kampf, C.J., Weber, B., Huffman, J.A., Pöhlker, C., Andreae, M.O.,
978 Lang-Yona, N., Burrows, S.M., Gunthe, S.S., Elbert, W., Su, H., Hoor, P., Thines, E.,

Hoffmann, T., Després, V.R., Pöschl, U., 2016. Bioaerosols in the Earth system: Climate, health, and ecosystem interactions. Atmospheric Res. 182, 346–376. https://doi.org/10.1016/j.atmosres.2016.07.018

Fu, P., Zhuang, G., Sun, Y., Wang, Q., Chen, J., Ren, L., Yang, F., Wang, Z., Pan, X., Li, X., Kawamura, K., 2016. Molecular markers of biomass burning, fungal spores and biogenic SOA in the Taklimakan desert aerosols. Atmos. Environ. 130, 64–73. https://doi.org/10.1016/j.atmosenv.2015.10.087

Gobierno Autonomo Descentralizado de la Provincia de Esmeraldas (GADPE), 2017. Prefectura de Esmeraldas. Ecuador http://www.prefecturadeesmeraldas.gob.ec/web/index.html.

Gilardoni, S., Vignati, E., Marmer, E., Cavalli, F., Belis, C., Gianelle, V., Loureiro, A., Artaxo, P., 2011. Sources of carbonaceous aerosol in the Amazon basin. Atmospheric Chem. Phys. 11, 2747–2764. https://doi.org/10.5194/acp-11-2747-2011

Graber, E.R., Rudich, Y., 2006. Atmospheric HULIS: How humic-like are they? A comprehensive and critical review. Atmospheric Chem. Phys. 6, 729–753. https://doi.org/10.5194/acp-6-729-2006

Guerreiro, C.B.B., Foltescu, V., de Leeuw, F., 2014. Air quality status and trends in Europe. Atmos. Environ. 98, 376–384. https://doi.org/10.1016/j.atmosenv.2014.09.017

Guinot, B., Cachier, H., Oikonomou, K., 2007. Geochemical perspectives from a new aerosol chemical mass closure. Atmospheric Chem. Phys. 7, 1657–1670. https://doi.org/10.5194/acp-7-1657-2007

Gurjar, B.R., Ravindra, K., Nagpure, A.S., 2016. Air pollution trends over Indian megacities and their local-to-global implications. Atmos. Environ. 142, 475–495. https://doi.org/10.1016/j.atmosenv.2016.06.030

Hadidi, L.A., AlDosary, A.S., Al-Matar, A.K., Mudallah, O.A., 2016. An optimization model to improve gas emission mitigation in oil refineries. J. Clean. Prod. 118, 29–36. https://doi.org/10.1016/j.jclepro.2016.01.033

Hedayat, F., Stevanovic, S., Miljevic, B., Bottle, S., Ristovski, Z.D., 2015. Review-evaluating the molecular assays for measuring the oxidative potential of particulate matter. Chem. Ind. Chem. Eng. Q. 21, 201–210. https://doi.org/10.2298/CICEQ140228031H

Hoek, G., Krishnan, R.M., Beelen, R., Peters, A., Ostro, B., Brunekreef, B., Kaufman, J.D., 2013. Long-term air pollution exposure and cardio- respiratory mortality: a review. Environ. Health 12. https://doi.org/10.1186/1476-069X-12-43

Huang, W., Zhang, Yuanxun, Zhang, Yang, Fang, D., Schauer, J.J., 2016. Optimization of the measurement of particle-bound reactive oxygen species with 2′,7′-dichlorofluorescin (DCFH). Water. Air. Soil Pollut. 227, 164. https://doi.org/10.1007/s11270-016-2860-9

Humood, M., Ghamary, M.H., Lan, P., Iaccino, L.L., Bao, X., Polycarpou, A.A., 2019. Influence of additives on the friction and wear reduction of oil-based drilling fluid. Wear 422–423, 151–160. https://doi.org/10.1016/j.wear.2019.01.028

Idelchik, M. del P.S., Begley, U., Begley, T.J., Melendez, J.A., 2017. Mitochondrial ROS control of cancer. Semin. Cancer Biol. https://doi.org/10.1016/j.semcancer.2017.04.005

Instituto Nacional de Meteorología e Hidrología (INAMHI), 2015. Anuario Meteorológico del Ecuador. N°52-2012. http://www.serviciometeorologico.gob.ec/wp-content/uploads/anuarios/meteorologicos/Am%202012.pdf.

Islam, R., Chhetri, A.B., Khan, M.M., 2010. The greening of petroleum operations. Wiley ; Scrivener Pub, Hoboken, N.J. : Salem, Mass.

Kelly, F.J., Fuller, G.W., Walton, H.A., Fussell, J.C., 2012. Monitoring air pollution: Use of early warning systems for public health: Monitoring and communicating air quality. Respirology 17, 7–19. https://doi.org/10.1111/j.1440-1843.2011.02065.x

Kirkhus, N.E., Thomassen, Y., Ulvestad, B., Woldbæk, T., Ellingsen, D.G., 2015. Occupational exposure to airborne contaminants during offshore oil drilling. Env. Sci Process. Impacts 17, 1257–1264. https://doi.org/10.1039/C5EM00081E

Krauss, M., Wilcke, W., Martius, C., Bandeira, A.G., Garcia, M.V.B., Amelung, W., 2005. Atmospheric versus biological sources of polycyclic aromatic hydrocarbons (PAHs) in

a tropical rain forest environment. Environ. Pollut. 135, 143–154. https://doi.org/10.1016/j.envpol.2004.09.012

Lessmann, J., Fajardo, J., Muñoz, J., Bonaccorso, E., 2016. Large expansion of oil industry in the Ecuadorian Amazon: biodiversity vulnerability and conservation alternatives. Ecol. Evol. 6, 4997–5012. https://doi.org/10.1002/ece3.2099

Lewis, R.C., Gaffney, S.H., Le, M.H., Unice, K.M., Paustenbach, D.J., 2012. Airborne concentrations of metals and total dust during solid catalyst loading and unloading operations at a petroleum refinery. Int. J. Hyg. Environ. Health 215, 514–521. https://doi.org/10.1016/j.ijheh.2011.10.006

Li, N., Sioutas, C., Cho, A., Schmitz, D., Misra, C., Sempf, J., Wang, M., Oberley, T., Froines, J., Nel, A., 2002. Ultrafine particulate pollutants induce oxidative stress and Mitochondrial Damage. Environ. Health Perspect. 111, 455–460. https://doi.org/10.1289/ehp.6000

Li, W., Wang, C., Shen, H., Su, S., Shen, G., Huang, Y., Zhang, Y., Chen, Y., Chen, H., Lin, N., Zhuo, S., Zhong, Q., Wang, X., Liu, J., Li, B., Liu, W., Tao, S., 2015. Concentrations and origins of nitro-polycyclic aromatic hydrocarbons and oxy-polycyclic aromatic hydrocarbons in ambient air in urban and rural areas in northern China. Environ. Pollut. 197, 156–164. https://doi.org/10.1016/j.envpol.2014.12.019

Liang, C.-S., Duan, F.-K., He, K.-B., Ma, Y.-L., 2016. Review on recent progress in observations, source identifications and countermeasures of PM2.5. Environ. Int. 86, 150–170. https://doi.org/10.1016/j.envint.2015.10.016

Malm, W.C., Schichtel, B.A., Pitchford, M.L., 2011. Uncertainties in PM2.5 gravimetric and speciation measurements and what we can learn from them. J. Air Waste Manag. Assoc. 61, 1131–1149. https://doi.org/10.1080/10473289.2011.603998

Martin, S.T., Andreae, M.O., Artaxo, P., Baumgardner, D., Chen, Q., Goldstein, A.H., Guenther, A., Heald, C.L., Mayol-Bracero, O.L., McMurry, P.H., Pauliquevis, T., Pöschl, U., Prather, K.A., Roberts, G.C., Saleska, S.R., Silva Dias, M.A., Spracklen, D.V., Swietlicki, E., Trebs, I., 2010. Sources and properties of Amazonian aerosol particles. Rev. Geophys. 48. https://doi.org/10.1029/2008RG000280

McDaniel, C.R., Jamison, D.E., 2014. Methods for use of oil-soluble weighting agents in subterranean formation treatment fluids. Google Patents.

Medeiros, P.M., Conte, M.H., Weber, J.C., Simoneit, B.R.T., 2006. Sugars as source indicators of biogenic organic carbon in aerosols collected above the Howland Experimental Forest, Maine. Atmos. Environ. 40, 1694–1705. https://doi.org/10.1016/j.atmosenv.2005.11.001

Mironenko, O.O., Sosnin, G.A., Eletskii, P.M., Gulyaeva, Yu.K., Bulavchenko, O.A., Stonkus, O.A., Rodina, V.O., Yakovlev, V.A., 2017. A study of the catalytic steam cracking of heavy crude oil in the presence of a dispersed molybdenum-containing catalyst. Pet. Chem. 57, 618–629. https://doi.org/10.1134/S0965544117070088

Monks, P.S., Granier, C., Fuzzi, S., Stohl, A., Williams, M.L., Akimoto, H., Amann, M., Baklanov, A., Baltensperger, U., Bey, I., Blake, N., Blake, R.S., Carslaw, K., Cooper, O.R., Dentener, F., Fowler, D., Fragkou, E., Frost, G.J., Generoso, S., Ginoux, P., Grewe, V., Guenther, A., Hansson, H.C., Henne, S., Hjorth, J., Hofzumahaus, A., Huntrieser, H., Isaksen, I.S.A., Jenkin, M.E., Kaiser, J., Kanakidou, M., Klimont, Z., Kulmala, M., Laj, P., Lawrence, M.G., Lee, J.D., Liousse, C., Maione, M., McFiggans, G., Metzger, A., Mieville, A., Moussiopoulos, N., Orlando, J.J., O'Dowd, C.D., Palmer, P.I., Parrish, D.D., Petzold, A., Platt, U., Pöschl, U., Prévôt, A.S.H., Reeves, C.E., Reimann, S., Rudich, Y., Sellegri, K., Steinbrecher, R., Simpson, D., ten Brink, H., Theloke, J., van der Werf, G.R., Vautard, R., Vestreng, V., Vlachokostas, Ch., von Glasow, R., 2009. Atmospheric composition change – global and regional air quality. Atmos. Environ. 43, 5268–5350. https://doi.org/10.1016/j.atmosenv.2009.08.021

Moreno, T., Pérez, N., Querol, X., Amato, F., Alastuey, A., Bhatia, R., Spiro, B., Hanvey, M., Gibbons, W., 2010. Physicochemical variations in atmospheric aerosols recorded at sea onboard the Atlantic–Mediterranean 2008 Scholar Ship cruise (Part II): Natural

versus anthropogenic influences revealed by PM10 trace element geochemistry. Atmos. Environ. 44, 2563–2576. https://doi.org/10.1016/j.atmosenv.2010.04.027

Mosandl, R., Günter, S., Stimm, B., Weber, M., 2008. Ecuador Suffers the Highest Deforestation Rate in South America, in: Beck, E., Bendix, J., Kottke, I., Makeschin, F., Mosandl, Reinhard (Eds.), Gradients in a Tropical Mountain Ecosystem of Ecuador. Springer Berlin Heidelberg, Berlin, Heidelberg, pp. 37–40.

National Toxicology Program (NTP), 2016. Report on Carcinogens, Fourteenth Edition. Research Triangle Park, NC: U.S. Department of Health and Human Services, Public Health Service.

Oliveira, C., Pio, C., Alves, C., Evtyugina, M., Santos, P., Gonçalves, V., Nunes, T., Silvestre, A.J.D., Palmgren, F., Wåhlin, P., Harrad, S., 2007. Seasonal distribution of polar organic compounds in the urban atmosphere of two large cities from the North and South of Europe. Atmos. Environ. 41, 5555–5570. https://doi.org/10.1016/j.atmosenv.2007.03.001

Oskarsson, A., 2015. Barium, in: Handbook on the Toxicology of Metals. Elsevier, pp. 625–634. https://doi.org/10.1016/B978-0-444-59453-2.00029-9

Ossés de Eicker, M., Hischier, R., Hurni, H., Zah, R., 2010. Using non-local databases for the environmental assessment of industrial activities: The case of Latin America. Environ. Impact Assess. Rev. 30, 145–157. https://doi.org/10.1016/j.eiar.2009.08.003

Palacios Espinoza, E., Espinoza Molina, C., 2014. Contaminación del aire exterior. Cuenca-Ecuador, 2009 -2013. Posibles efectos en la salud. Rev. Fac. Cienc. Médicas Univ. Cuenca 32, 6–17.

Perraudin, E., Budzinski, H., Villenave, E., 2005. Analysis of polycyclic aromatic hydrocarbons adsorbed on particles of atmospheric interest using pressurised fluid extraction. Anal. Bioanal. Chem. 383, 122–131. https://doi.org/10.1007/s00216-005-3398-7

Perrone, M.G., Gualtieri, M., Consonni, V., Ferrero, L., Sangiorgi, G., Longhin, E., Ballabio, D., Bolzacchini, E., Camatini, M., 2013. Particle size, chemical composition, seasons of the year and urban, rural or remote site origins as determinants of biological effects of particulate matter on pulmonary cells. Environ. Pollut. 176, 215–227. https://doi.org/10.1016/j.envpol.2013.01.012

Pey, J., Pérez, N., Cortés, J., Alastuey, A., Querol, X., 2013. Chemical fingerprint and impact of shipping emissions over a western Mediterranean metropolis: Primary and aged contributions. Sci. Total Environ. 463–464, 497–507. https://doi.org/10.1016/j.scitotenv.2013.06.061

Philip, S., Martin, R.V., Pierce, J.R., Jimenez, J.L., Zhang, Q., Canagaratna, M.R., Spracklen, D.V., Nowlan, C.R., Lamsal, L.N., Cooper, M.J., Krotkov, N.A., 2014. Spatially and seasonally resolved estimate of the ratio of organic mass to organic carbon. Atmos. Environ. 87, 34–40. https://doi.org/10.1016/j.atmosenv.2013.11.065

Pourrut, P., 1995. El Agua en el Ecuador. Clima, precipitaciones, escorrentía, Estudios de Geografía. Corporación Editora Nacional. Colegio de Geógrafos del Ecuador.

Pradhan, D., Patra, A.K., Kim, D.-J., Chung, H.-S., Lee, S.-W., 2013. A novel sequential process of bioleaching and chemical leaching for dissolving Ni, V, and Mo from spent petroleum refinery catalyst. Hydrometallurgy 131–132, 114–119. https://doi.org/10.1016/j.hydromet.2012.11.004

Raaschou-Nielsen, O., Andersen, Z.J., Beelen, R., Samoli, E., Stafoggia, M., Weinmayr, G., Hoffmann, B., Fischer, P., Nieuwenhuijsen, M.J., Brunekreef, B., Xun, W.W., Katsouyanni, K., Dimakopoulou, K., Sommar, J., Forsberg, B., Modig, L., Oudin, A., Oftedal, B., Schwarze, P.E., Nafstad, P., De Faire, U., Pedersen, N.L., Östenson, C.-G., Fratiglioni, L., Penell, J., Korek, M., Pershagen, G., Eriksen, K.T., Sørensen, M., Tjønneland, A., Ellermann, T., Eeftens, M., Peeters, P.H., Meliefste, K., Wang, M., Bueno-de-Mesquita, B., Key, T.J., de Hoogh, K., Concin, H., Nagel, G., Vilier, A., Grioni, S., Krogh, V., Tsai, M.-Y., Ricceri, F., Sacerdote, C., Galassi, C., Migliore, E., Ranzi, A., Cesaroni, G., Badaloni, C., Forastiere, F., Tamayo, I., Amiano, P., Dorronsoro, M., Trichopoulou, A., Bamia, C., Vineis, P., Hoek, G., 2013. Air pollution and lung cancer incidence in 17 European cohorts: prospective analyses from the

European Study of Cohorts for Air Pollution Effects (ESCAPE). Lancet Oncol. 14, 813–822. https://doi.org/10.1016/S1470-2045(13)70279-1

Red Amazónica de Información Socio ambiental Georreferenciada (RAIS, 2015. Deforestación en la Amazonia (1970-2013). 48 pags. www.raisg.socioambiental.org

Raysoni, A., Armijos, R., Weigel, M., Echanique, P., Racines, M., Pingitore, N., Li, W.-W., 2017. Evaluation of Sources and Patterns of Elemental Composition of PM2.5 at Three Low-Income Neighborhood Schools and Residences in Quito, Ecuador. Int. J. Environ. Res. Public. Health 14, 674. https://doi.org/10.3390/ijerph14070674

Raysoni, A.U., Armijos, R.X., Weigel, M.M., Montoya, T., Eschanique, P., Racines, M., Li, W.-W., 2016. Assessment of indoor and outdoor PM species at schools and residences in a high-altitude Ecuadorian urban center. Environ. Pollut. 214, 668–679. https://doi.org/10.1016/j.envpol.2016.04.085

Reche, C., Viana, M., Amato, F., Alastuey, A., Moreno, T., Hillamo, R., Teinilä, K., Saarnio, K., Seco, R., Peñuelas, J., Mohr, C., Prévôt, A.S.H., Querol, X., 2012. Biomass burning contributions to urban aerosols in a coastal Mediterranean City. Sci. Total Environ. 427–428, 175–190. https://doi.org/10.1016/j.scitotenv.2012.04.012

Ringuet, J., Albinet, A., Leoz-Garziandia, E., Budzinski, H., Villenave, E., 2012. Diurnal/nocturnal concentrations and sources of particulate-bound PAHs, OPAHs and NPAHs at traffic and suburban sites in the region of Paris (France). Sci. Total Environ. 437, 297–305. https://doi.org/10.1016/j.scitotenv.2012.07.072

Rudel, T.K., Bates, D., Machinguiashi, R., 2002. A Tropical Forest Transition? Agricultural Change, Out-migration, and Secondary Forests in the Ecuadorian Amazon. Ann. Assoc. Am. Geogr. 92, 87–102. https://doi.org/10.1111/1467-8306.00281

Saffari, A., Daher, N., Shafer, M.M., Schauer, J.J., Sioutas, C., 2014. Global Perspective on the Oxidative Potential of Airborne Particulate Matter: A Synthesis of Research Findings. Environ. Sci. Technol. 48, 7576–7583. https://doi.org/10.1021/es500937x

Samaké, A., Jaffrezo, J.-L., Favez, O., Weber, S., Jacob, V., Albinet, A., Riffault, V., Perdrix, E., Waked, A., Golly, B., Salameh, D., Chevrier, F., Oliveira, D.M., Bonnaire, N., Besombes, J.-L., Martins, J.M.F., Conil, S., Guillaud, G., Mesbah, B., Rocq, B., Robic, P.-Y., Hulin, A., Le Meur, S., Descheemaecker, M., Chretien, E., Marchand, N., Uzu, G., 2019a. Polyols and glucose particulate species as tracers of primary biogenic organic aerosols at 28 French sites. Atmospheric Chem. Phys. 19, 3357–3374. https://doi.org/10.5194/acp-19-3357-2019

Samaké, A., Jaffrezo, J.-L., Favez, O., Weber, S., Jacob, V., Canete, T., Albinet, A., Charron, A., Riffault, V., Perdrix, E., Waked, A., Golly, B., Salameh, D., Chevrier, F., Oliveira, D.M., Besombes, J.-L., Martins, J.M.F., Bonnaire, N., Conil, S., Guillaud, G., Mesbah, B., Rocq, B., Robic, P.-Y., Hulin, A., Le Meur, S., Descheemaecker, M., Chretien, E., Marchand, N., Uzu, G., 2019b. Arabitol, mannitol, and glucose as tracers of primary biogenic organic aerosol: the influence of environmental factors on ambient air concentrations and spatial distribution over France. Atmospheric Chem. Phys. 19, 11013–11030. https://doi.org/10.5194/acp-19-11013-2019

Samaké, A., Uzu, G., Martins, J.M.F., Calas, A., Vince, E., Parat, S., Jaffrezo, J.L., 2017. The unexpected role of bioaerosols in the Oxidative Potential of PM. Sci. Rep. 7. https://doi.org/10.1038/s41598-017-11178-0

San Sebastián, M., Armstrong, J., Córdova, J.A., Stephens, C., 2001. Exposures and cancer incidence near oil fields in the Amazon basin of Ecuador. Occup. Environ. Med. 58, 517–522. https://doi.org/10.1136/oem.58.8.517

San Sebastián, M., Hurtig, A.K., 2005. Oil development and health in the Amazon basin of Ecuador: the popular epidemiology process. Soc. Sci. Med. 60, 799–807. https://doi.org/10.1016/j.socscimed.2004.06.016

San Sebastián, M., Hurtig, A.-K., 2004. Oil exploitation in the Amazon basin of Ecuador: a public health emergency. Rev. Panam. Salud Pública 15. https://doi.org/10.1590/S1020-49892004000300014

Santibáñez-Andrade, M., Quezada-Maldonado, E.M., Osornio-Vargas, Á., Sánchez-Pérez, Y., García-Cuellar, C.M., 2017. Air pollution and genomic instability: The role of particulate

matter in lung carcinogenesis. Environ. Pollut. 229, 412–422. https://doi.org/10.1016/j.envpol.2017.06.019

Santos, F., Fraser, M.P., Bird, J.A., 2014. Atmospheric black carbon deposition and characterization of biomass burning tracers in a northern temperate forest. Atmos. Environ. 95, 383–390. https://doi.org/10.1016/j.atmosenv.2014.06.038

Sarnela, N., Jokinen, T., Nieminen, T., Lehtipalo, K., Junninen, H., Kangasluoma, J., Hakala, J., Taipale, R., Schobesberger, S., Sipilä, M., Larnimaa, K., Westerholm, H., Heijari, J., Kerminen, V.-M., Petäjä, T., Kulmala, M., 2015. Sulphuric acid and aerosol particle production in the vicinity of an oil refinery. Atmos. Environ. 119, 156–166. https://doi.org/10.1016/j.atmosenv.2015.08.033

Sauvain, J.-J., Rossi, M.J., Riediker, M., 2013. Comparison of three acellular tests for assessing the oxidation potential of nanomaterials. Aerosol Sci. Technol. 47, 218–227. https://doi.org/10.1080/02786826.2012.742951

Schock, B.C., Koostra, J., Kwack, S., Hackman, R.M., van der Vliet, A., Cross, C.E., 2004. Ascorbic acid in nasal and tracheobronchial airway lining fluids. Free Radic. Biol. Med. 37, 1393–1401. https://doi.org/10.1016/j.freeradbiomed.2004.07.023

Schreck, E., Sarret, G., Oliva, P., Calas, A., Sobanska, S., Guédron, S., Barraza, F., Point, D., Huayta, C., Couture, R.-M., Prunier, J., Henry, M., Tisserand, D., Goix, S., Chincheros, J., Uzu, G., 2016. Is Tillandsia capillaris an efficient bioindicator of atmospheric metal and metalloid deposition? Insights from five months of monitoring in an urban mining area. Ecol. Indic. 67, 227–237. https://doi.org/10.1016/j.ecolind.2016.02.027

Scipioni, C., Villanueva, F., Pozo, K., Mabilia, R., 2012. Preliminary characterization of polycyclic aromatic hydrocarbons, nitrated polycyclic aromatic hydrocarbons and polychlorinated dibenzo-p-dioxins and furans in atmospheric PM10 of an urban and a remote area of Chile. Environ. Technol. 33, 809–820. https://doi.org/10.1080/09593330.2011.597433

Secrest, M.H., Schauer, J.J., Carter, E.M., Lai, A.M., Wang, Y., Shan, M., Yang, X., Zhang, Y., Baumgartner, J., 2016. The oxidative potential of PM2.5 exposures from indoor and outdoor sources in rural China. Sci. Total Environ. 571, 1477–1489. https://doi.org/10.1016/j.scitotenv.2016.06.231

Secretaría De Hidrocarburos Ecuador (SHE), 2015. Ministerio de Recursos Naturales No Renovables.

Subsistema Multidimensional de Estadísticas Socio Ambientales de las Actividades Productivas (SIESAP), 2015. Programa de Reparación Ambiental y Social (PRAS). Ministerio del Ambiente de Ecuador http://pras.ambiente.gob.ec/web/siesap/informacion-eh.

Squadrito, G.L., Cueto, R., Dellinger, B., Pryor, W.A., 2001. Quinoid redox cycling as a mechanism for sustained free radical generation by inhaled airborne particulate matter. Free Radic. Biol. Med. 31, 1132–1138. https://doi.org/10.1016/S0891-5849(01)00703-1

Szigeti, T., Óvári, M., Dunster, C., Kelly, F.J., Lucarelli, F., Záray, G., 2015. Changes in chemical composition and oxidative potential of urban PM2.5 between 2010 and 2013 in Hungary. Sci. Total Environ. 518–519, 534–544. https://doi.org/10.1016/j.scitotenv.2015.03.025

Verma, V., Ning, Z., Cho, A.K., Schauer, J.J., Shafer, M.M., Sioutas, C., 2009. Redox activity of urban quasi-ultrafine particles from primary and secondary sources. Atmos. Environ. 43, 6360–6368. https://doi.org/10.1016/j.atmosenv.2009.09.019

Visentin, M., Pagnoni, A., Sarti, E., Pietrogrande, M.C., 2016. Urban PM2.5 oxidative potential: Importance of chemical species and comparison of two spectrophotometric cell-free assays. Environ. Pollut. 219, 72–79. https://doi.org/10.1016/j.envpol.2016.09.047

Waked, A., Favez, O., Alleman, L.Y., Piot, C., Petit, J.-E., Delaunay, T., Verlinden, E., Golly, B., Besombes, J.-L., Jaffrezo, J.-L., Leoz-Garziandia, E., 2014. Source apportionment of PM10 in a north-western Europe regional urban background site (Lens, France) using positive matrix factorization and including primary biogenic emissions. Atmospheric Chem. Phys. 14, 3325–3346. https://doi.org/10.5194/acp-14-3325-2014

Weber, S., Gaëlle, U., Calas, A., Chevrier, F., Besombes, J.-L., Charron, A., Salameh, D., Ježek, I., Močnik, G., Jaffrezo, J.-L., 2018. An apportionment method for the Oxydative Potential to the atmospheric PM sources: application to a one-year study in Chamonix, France. Atmospheric Chem. Phys. Discuss. 1–19. https://doi.org/10.5194/acp-2017-1053

Welford, M.R., Yarbrough, R.A., 2015. Serendipitous conservation: Impacts of oil pipeline construction in rural northwestern Ecuador. Extr. Ind. Soc. 2, 766–774. https://doi.org/10.1016/j.exis.2015.07.005

Yamasoe, M.A., Artaxo, P., Miguel, A.H., Allen, A.G., 2000. Chemical composition of aerosol particles from direct emissions of vegetation fires in the Amazon Basin: water-soluble species and trace elements. Atmos. Environ. 34, 1641–1653. https://doi.org/10.1016/S1352-2310(99)00329-5

Yang, A., Jedynska, A., Hellack, B., Kooter, I., Hoek, G., Brunekreef, B., Kuhlbusch, T.A.J., Cassee, F.R., Janssen, N.A.H., 2014. Measurement of the oxidative potential of PM2.5 and its constituents: The effect of extraction solvent and filter type. Atmos. Environ. 83, 35–42. https://doi.org/10.1016/j.atmosenv.2013.10.049

Yang, Z., Wang, J., 2017. A new air quality monitoring and early warning system: Air quality assessment and air pollutant concentration prediction. Environ. Res. 158, 105–117. https://doi.org/10.1016/j.envres.2017.06.002

Yassaa, N., Cecinato, A., 2005. Composition of torched crude oil organic particulate emitted by refinery and its similarity to atmospheric aerosol in the surrounding area. Chemosphere 60, 1660–1666. https://doi.org/10.1016/j.chemosphere.2005.02.041

Zhang, Z., Wang, H., Chen, D., Li, Q., Thai, P., Gong, D., Li, Y., Zhang, C., Gu, Y., Zhou, L., Morawska, L., Wang, B., 2017. Emission characteristics of volatile organic compounds and their secondary organic aerosol formation potentials from a petroleum refinery in Pearl River Delta, China. Sci. Total Environ. 584–585, 1162–1174. https://doi.org/10.1016/j.scitotenv.2017.01.179

Zhao, M., Qiao, T., Li, Y., Tang, X., Xiu, G., Yu, J.Z., 2016. Temporal variations and source apportionment of Hulis-C in PM2.5 in urban Shanghai. Sci. Total Environ. 571, 18–26. https://doi.org/10.1016/j.scitotenv.2016.07.127

Zhu, C., Kawamura, K., Kunwar, B., 2015. Effect of biomass burning over the western North Pacific Rim: wintertime maxima of anhydrosugars in ambient aerosols from Okinawa. Atmospheric Chem. Phys. 15, 1959–1973. https://doi.org/10.5194/acp-15-1959-2015

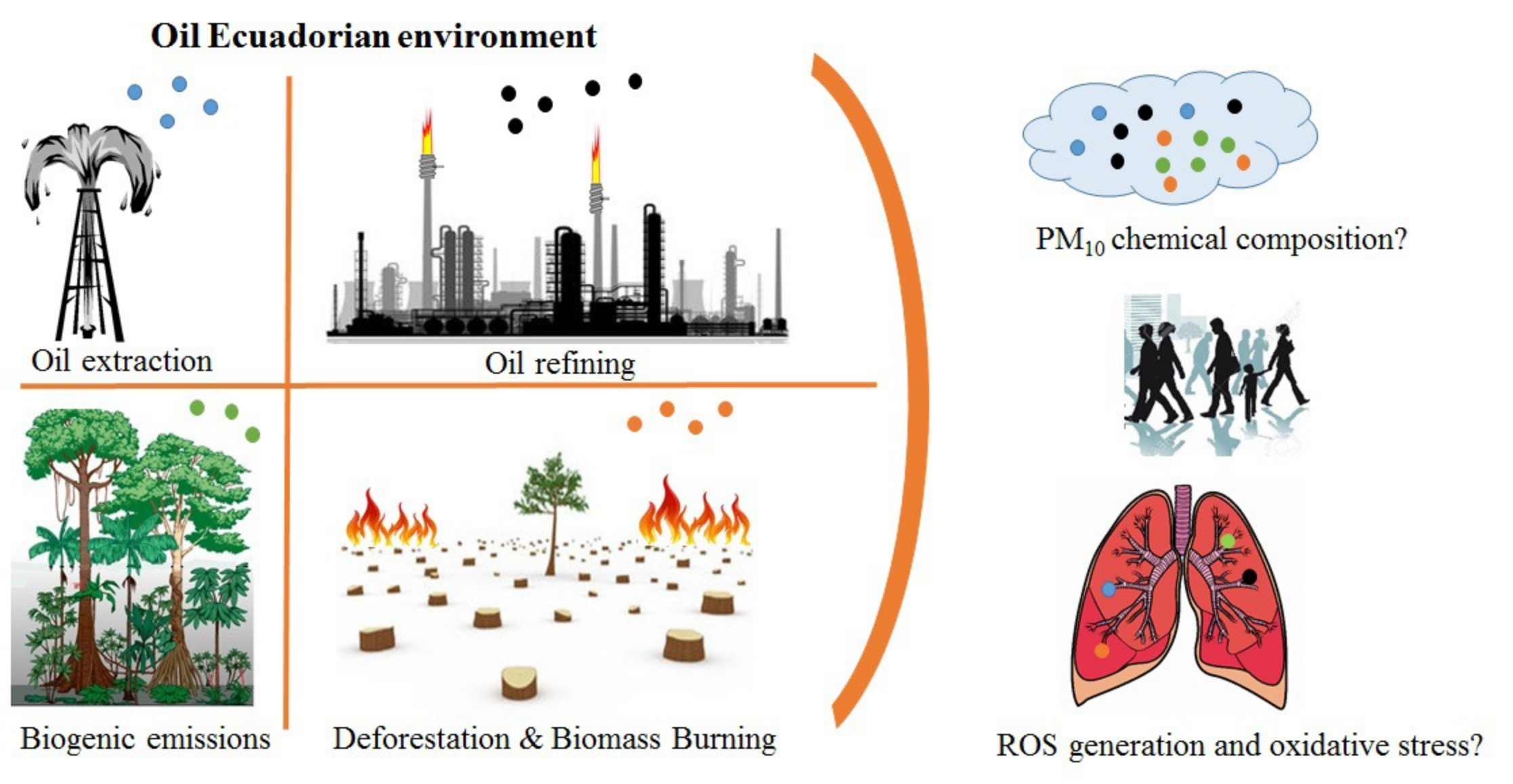
Oil Ecuadorian environment
Oil extraction
Oil refining
Biogenic emissions
Deforestation & Biomass Burning
PM10 chemical composition?
ROS generation and oxidative stress?